Author manuscript of article published in Polymer Chemistry (2023) https://doi.org/10.1039/D2PY01318E

Unveiling the reactivity of epoxides in carbonated epoxidized soybean oil and application to the stepwise synthesis of hybrid poly(hydroxyurethane) thermosets

P. Helbling[1,2], F. Hermant[2], M. Petit[2], T. Tassaing[3], T. Vidil[1] and H. Cramail[1*]*

[1]Univ. Bordeaux, CNRS, Bordeaux INP, LCPO, 16 avenue Pey-Berland 33600 Pessac, France

[2]Saint-Gobain Recherche Paris, 39 Quai Lucien Lefranc 93300 Aubervilliers, France

[3]Univ. Bordeaux, CNRS, Bordeaux INP, ISM, 351 cours de la Libération 33405 Talence, France

Abstract

In this work, the crosslinking reaction of partially carbonated epoxidized soybean oils with different diamines was investigated. To this end, a series of carbonated soybean oils (CSBO), with a carbonation ratio ranging from 45 % (CSBO45) to 98 % (CSBO98) were synthesized by CO_2-carbonation of epoxidized soybean oil (ESBO). The relative aminolysis rate of carbonate and epoxide functions of CSBO45, but also of the esters of the triglyceride skeleton, was monitored through an unprecedented combination of *in-situ* infrared and Raman spectroscopy at various temperatures T, 60 °C ≤ T ≤ 150 °C. Interestingly, two regimes are identified: (i) for T < 100 °C, a *PHU regime*, during which all the carbonate functions of CSBO45 react to provide an uncrosslinked PHU prepolymer (viscous liquid), (ii) for T ≥ 100 °C, a *hybrid regime*, during which the epoxide functions react to provide a hybrid thermosetting polymer (elastic solid). For the first time, we report the "conversion *vs* time" plots for the aminolysis of epoxide in ESBO and partially carbonated ESBO. They indicate that the initiation of the reaction is thermally delayed as compared to the aminolysis of the corresponding carbonates. Surprisingly, the sol-gel transition of CSBO45 is correlated to the initiation of the epoxides aminolysis, a counterintuitive conclusion given that ESBO cannot be crosslinked by a diamine in the same conditions. These results suggest that the combination of reactive carbonates with sluggish epoxides results in a decrease of undesirable side reactions such as ester aminolysis and intramolecular cyclization. Finally, general guidelines can be recommended for the stepwise synthesis of triglyceride-based hybrid poly(hydroxyurethane) thermosets.

Introduction

Polyurethane (PU) synthesis, involving polyols and polyisocyanates, is nowadays ubiquitous as it is used in a very broad range of applications, from foams to coatings to name a few.[1] According to PlasticsEurope, the European demand in PUs reached 3.81 million tons in 2020, representing 8 % of the overall polymer materials demand.[2] Even though the polyol route to PUs is robust and these materials are irreplaceable for everyday-life products, the use of toxic diisocyanates for their synthesis represents a significant environmental and health hazard. Indeed, in addition of being mainly derived from fossil resources, most of the diisocyanates used in the industry are now registered as hazardous chemicals by the REACH regulation. In fact, a recent amendment to the regulation published by the European Commission will soon drastically limit their use as reactants if no safety measures are taken in manufacturing plants.[3]

These reasons lead to the development of greener alternative PU syntheses, with the aim to find chemical pathways suitable for an industrial scale production. Among the different non-isocyanate polyurethanes (NIPUs) synthetic pathways, the cyclic carbonate-amine reaction leading to polyhydroxyurethanes (PHUs) has been the most developed; it is a polyaddition reaction, thus releasing no by-product, and the reactants can be easily biobased and are mostly non-toxic.[4–6] In this sense, different biobased compounds such as vegetable oils and fatty acids,[7–13] glycerol,[14–16] sugar-derived molecules[17–20] or terpenes[21–23] and lignin[24] have been derivatized to prepare either cyclic carbonates or amines to design PHUs with a large set of thermomechanical properties. Vegetable oils are particularly interesting as they are readily available in large amount, and they usually contain unsaturations that can be easily modified to obtain polyfunctional monomers. Thus, various vegetable oils such as soybean or linseed oils were epoxidized and then carbonated through the coupling of CO_2 with epoxides. Other oils like jojoba were modified through thiol-ene reaction to directly graft the cyclic carbonate moieties.[25–27]

The carbonation reaction of epoxidized vegetable oils has been widely studied and occurs generally at elevated temperature, under high CO_2 pressure or under supercritical conditions. Such reactions are conventionally catalysed by tetrabutylamonium bromide or iodide (TBAB or TBAI) while recent studies discussed the use of organocatalysts, ionic liquids or heterogeneous catalysts.[7,28–32] Most of the time, epoxidized vegetable oils are fully carbonated in order to improve the crosslinking rate and the thermo-mechanical properties of the PHU networks. Indeed, different studies suggested that residual epoxide functions of carbonated soybean oil do not react with amines during the crosslinking reaction thus affecting the final properties of the networks. Javni *et al*. observed that the crosslinking rate of a system composed of a partially carbonated epoxidized soybean oil and a diamine is lower than the one measured for a fully carbonated soybean oil.[33] The authors found out that the epoxy oxygen content of ESBO was mostly unchanged after being cured with various diamines and concluded that the residual epoxides on a carbonated soybean oil do not react with the diamine. In another study, Poussard *et al*. designed various

partially carbonated epoxidized soybean oils and studied their reaction with diamines at 120 °C for 3 h through rheology.[30] The authors observed that the evolution of the torque value was dependent on the amount of carbonate functions and was drastically increasing with the carbonate content. In any case, the torque value was higher when a carbonated soybean oil was used instead of the corresponding epoxidized soybean oil in the same conditions. Furthermore, the conversion of carbonate functions was confirmed with Fourier-Transform Infrared (FTIR) spectroscopy analyses when carbonated soybean oils were used while, in the case of epoxidized soybean oil, the characteristic band of epoxides did not show any change during the reaction. These results suggested that the carbonate-amine reaction was predominant over the epoxy-amine one and highlighted the rather low reactivity of epoxide functions in comparison to carbonates. Nevertheless, according to Liu *et al*., epoxides from epoxidized soybean oil are sufficiently reactive at temperatures higher than 160 °C to react with 4,4'-dithiophenylamine and lead to a thermoset.[34] Other authors also obtained thermosets from epoxidized soybean oil via the epoxy-amine reaction, highlighting the reactivity of epoxide functions.[35–38] Figovsky *et al*. synthesized partially carbonated-epoxidized soybean oil, with a carbonate content comprised between 35 and 85 %, in order to obtain hybrid PHU cured at room temperature, taking advantage of the reactivity of the remaining epoxide functions.[39,40] In this case, the cyclic carbonate-amine reaction is first exploited, suggesting that carbonates are more reactive than epoxides when partially carbonated epoxidized soybean oil is considered. The epoxy-amine reaction was then exploited in a second stage, which involved the epoxide functions of the oil and, in some cases, the ones of an external epoxidized compound added in the system.

Overall, although ESBO/CSBO-diamine systems are increasingly used in polymer chemistry, the understanding of the chemistry behind is still incomplete and a number of contradictory affirmations have been published in the literature. In particular, the kinetics of the reaction of the epoxide functions of ESBO (and partially carbonated ESBO) with diamines have never been studied comprehensively *via* a direct measuring method (conventional FTIR cannot be used in that case). The exact initiation temperatures and the *"conversion vs time"* plots have never been reported. In the end, the crosslinking conditions cannot be optimized based on this fragmentary knowledge of the epoxide reactivity.

In this study, we provide the first quantitative and comprehensive measurement of the epoxides aminolysis rate during the reaction of ESBO – and partially carbonated ESBO – with diamines thanks to the unprecedented use of Raman spectroscopy for the *in-situ* monitoring the crosslinking reaction. Furthermore, in the case of partially carbonated epoxidized soybean oils, the relative reactivity of cyclic carbonate and epoxide functions of partially carbonated epoxidized soybean oils with amines was quantitatively investigated thanks to the combination of IR and Raman spectroscopy. To this purpose, partially carbonated epoxidized soybean oils were cured at various temperatures with diamines (Priamine 1075 or 1,8-octanediamine) and the reactions were monitored through the above-mentioned combination of IR and Raman spectroscopy as well as rheology. For the first time, Raman spectroscopy provides unambiguous evidence of the involvement of the epoxide in the crosslinking reaction, in

contrast with the previous experimental approaches reported in the literature that were solely based on IR measurements. Advantageously, the dual spectroscopic monitoring of the reaction enables a precise discrimination of the initiation of the aminolysis of carbonates, epoxides, and esters as a function of temperature. As expected, their reactivities are ranged as follow, carbonates > epoxides > esters. More surprisingly, Raman spectroscopy combined with rheometric measurements indicates that the sol-gel transition of ESBO with a carbonation ratio of about 50 % relies on the initiation of the epoxide-amine reaction, a counterintuitive conclusion given that pristine ESBO cannot be crosslinked by a diamine in the same conditions. This result, together with reference experiments conducted on ESBO, suggests that the combination of reactive carbonates with sluggish epoxides leads to a decrease of undesirable side reactions including ester aminolysis and intramolecular cyclization. It sheds a brand-new light on the competitive reactions occurring in triglyceride-based thermosets and on their impact on the macromolecular topology of the growing network during the polymerization. From a practical standpoint, these findings are offering new guidelines for the optimization of the crosslinking reaction of partially carbonated epoxidized soybean oil with diamines. They indicate that a two-step crosslinking sequence, with a pre-polymerization in the *PHU regime* (T < 100 °C), followed by a completion of the reaction in the *Hybrid regime* (T > 100 °C), is optimal for an efficient polymerization of CSBO. Eventually, this stepwise crosslinking approach is of interest to control the rheological behavior of triglyceride-based materials during their manufacturing processes.

Experimental section

Materials

Epoxidized soybean oil ESBO (ITERG, 4.4 mol of epoxides kg^{-1}); Tetrabutylammonium bromide - TBAB (Aldrich, 99 %); Priamine 1075 (Croda, I_a = 206 mg KOH g^{-1}, M = 544.66 g mol^{-1}) degassed under vacuum prior to use; 1,8-octanediamine - 8DA (TCI, > 98 %); dimethyl sulfoxide-d_6 (DMSO-d_6) (99.8 % D); deuterated dichloromethane CD_2Cl_2 (99.9 % D); 1,2,4-trichlorobenzene (J.T. Baker, 99 %) dried over molecular sieve 4 Å prior to use.

Synthesis of partially carbonated soybean oils

The carbonated soybean oils (CSBO) were synthesized from epoxidized soybean oil (ESBO) through a one-step bulk procedure. ESBO (2.5 g) as well as the catalyst, TBAB (3 wt% relative to ESBO, i.e. ~ 2 mol% relative to the epoxide functions), were placed in a 22 mL reactor. The latter was pressurized with CO_2 (45 bar), heated at 120 °C and magnetically stirred (250 rpm) (see ESI, Figure S1). The time of reaction went from 8 to 72 h to obtain carbonation ratios ranging from 47 to 98 %. At the end of the reactions, the reactor was cooled down and slowly depressurized. The conversion of epoxide into carbonate functions, X, was determined thanks to ^{1}H NMR by dissolving the samples in CD_2Cl_2 or

DMSO-d_6 and using 1,2,4-trichlorobenzene as an internal reference (see ESI, Figure S2, S3 and Eq. S1, S2). A large batch (250 g) of partially carbonated ESBO with X = 45 % (CSBO45, see ESI Figure S4) was obtained by using a 500 mL reactor equipped with a mechanical stirrer. Carbonation proceeds according to the same protocol.

Synthesis of PHUs and monitoring of the crosslinking reaction

CSBO45 and the diamine, previously grinded in the case of 8DA, were mixed with a ratio $[NH_2]$ = [carbonate] + [epoxide]/2 by stirring with a spatula and then degassed. The crosslinking reactions were carried out at various temperatures between 60 and 150 °C. In each case, a portion of the mixture was used for *in-situ* IR and Raman spectroscopy monitoring and another part was poured in a mould in order to obtain a rectangular sample and carry out swelling tests and thermal analyses. The crosslinking reaction was additionally monitored by rheological analysis to study the sol-gel transition. The methods used to follow the conversions of the reactive functions and the gelation process are described in Electronic Supporting Information ESI-p. S8-S9.

Comparative experiments involving ESBO were also run at 120 and 150 °C with the ratio $[NH_2]$ = [epoxide]/2.

The structure of the epoxide and amine precursors used for the synthesis of PHUs are represented in Figure 1.

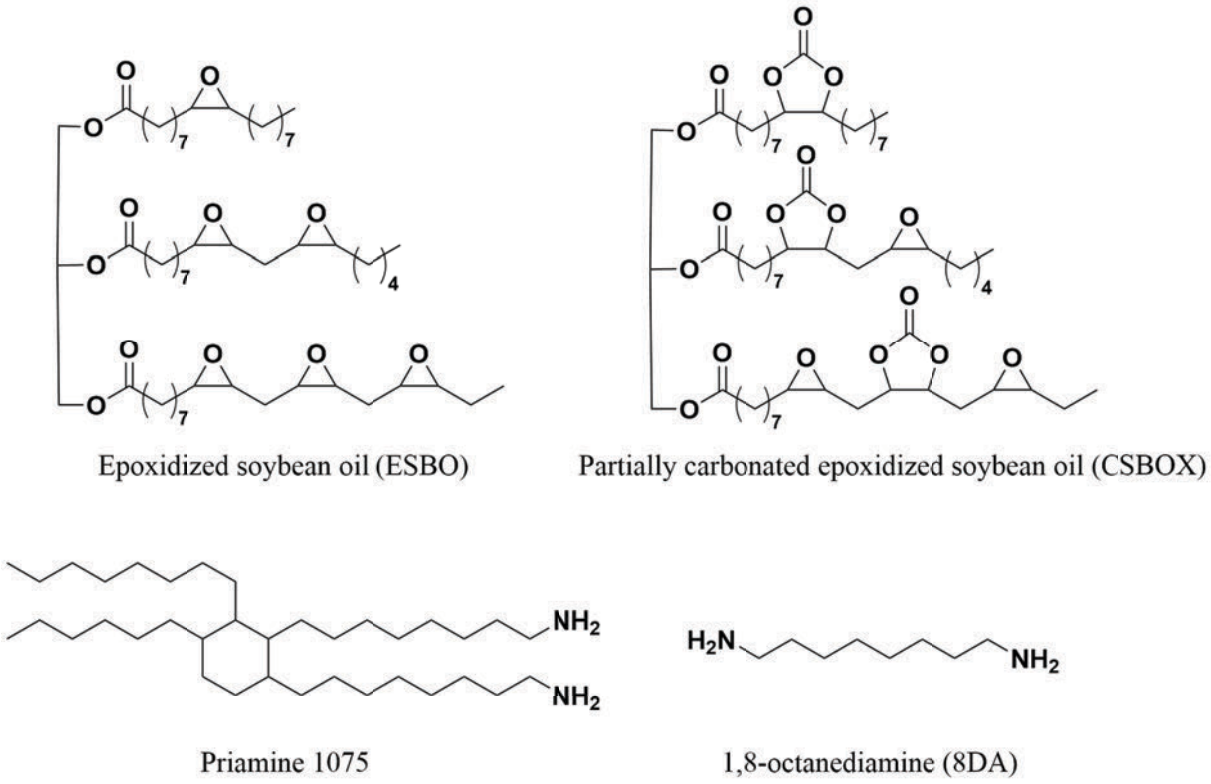

Figure 1 : Functional precursors investigated for the synthesis of the hybrid PHU networks – For both ESBO and CSBO one regio/stereo-isomer is represented as an example case

Swelling tests

Swelling tests were run at room temperature using toluene as solvent. The samples of mass m_0 (g) were immersed in toluene and were weighed each day for at least 1 week after removing the excess of solvent at their surface. The polymers were swollen until they reach a stable mass, m_s (g), for at least 3 consecutive mass measurements. At the end, the samples were dried at 40 °C under vacuum for 4 hours and weighed to measure the dry mass m_d (g). The remaining solvent containing the soluble fraction was also kept for further analyses.

The swelling ratio, Q (%), and the soluble fraction, w_{sol} (%), were calculated according to the Eq. 1 and Eq. 2, respectively:

$$\text{Eq. 1: } Q = \frac{m_s - m_d}{m_d} \times 100$$

$$\text{Eq. 2: } w_{sol} = \left(1 - \frac{m_d}{m_0}\right) \times 100$$

Results and discussion

Synthesis of partially carbonated ESBO: CSBOX

ESBO was carbonated under CO_2 pressurization at elevated temperature and the reaction was catalyzed by tetrabutylammonium bromide, TBAB. The conversion of epoxides into carbonates X – in other words the carbonate ratio – was measured at the end of the reaction according to ^{1}H NMR analyses. Based on a screening of the influence of the various parameters of the carbonation conditions (see the ESI, Figure S1), the reactions were carried out at T = 120 °C with an initial pressure of CO_2 $P_{CO2,\ init.}$ = 45 bar and a catalyst content of 3 wt% (magnetic stirring set at ω = 250 round per minute, rpm). Conveniently, with these conditions, it is possible to obtain a series of partially carbonated epoxidized soybean oils, CSBOX, with 47 % ≤ X ≤ 98 %, simply by varying the reaction time between 8 h and 72 h. Figure 2 represents the evolution of X as a function of the reaction time, X(t). Clearly, X(t) is an increasing function of the reaction time. Additionally, we observed that X(t) is dependent on the size of the reactor and the stirring mode. Thus, when the reaction is conducted in a 22 mL reactor under magnetic stirring, X(8h) = 47 %. On the other hand, when we tried to obtain large amount of CSBOX in a 500 mL reactor equipped with a mechanical stirrer, X(5h) = 45 %. Thus, under the same conditions (T = 120 °C, $P_{CO2,\ init.}$ = 45 bar, 3 wt% TBAB, ω = 250 rpm), the carbonation reaction seems to be much faster in the larger reactor. This is explained by considering the better efficiency of mechanical stirring in incorporating CO_2 into the viscous ESBO, thus facilitating the contact between the reactants.

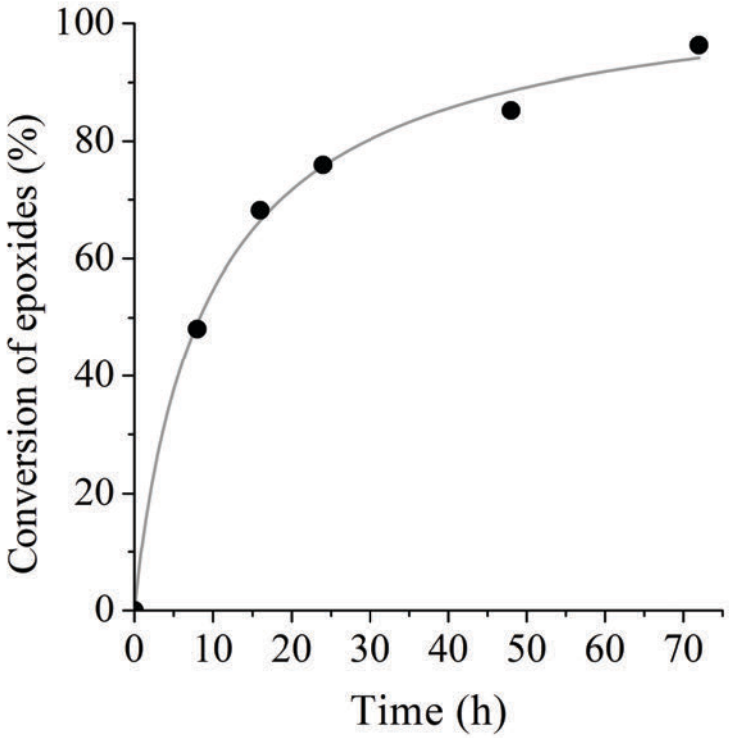

Figure 2: Conversion of epoxides, X, as a function of time for the carbonation reaction carried out at T = 120 °C, $P_{CO2,init.}$ = 45 bar of CO_2, 3 wt% TBAB and under magnetic stirring ω = 250 rpm

Dual-spectroscopic investigation of the crosslinking reaction of CSBO45

In the rest of the study, the investigation of the crosslinking reaction of the partially carbonated ESBO is focused on CSBO45. Indeed, in this case, the triglyceride contains approximately an equal number of carbonate and epoxide functions, thus facilitating the study of the relative aminolysis rate of both functions.

The crosslinking reaction of CSBO45, schematically represented in Figure 3, has been studied with two diamines: (i) a dimeric fatty diamine, well known under its commercial brand-name, Priamine 1075, which will be used in the rest of the paper and (ii) the 1,8-octanediamine (8DA). Advantageously, these two low-toxicity diamines are commercially available. Moreover, Priamine 1075 is derived from oleic and/or linoleic acid, meaning it is biobased.

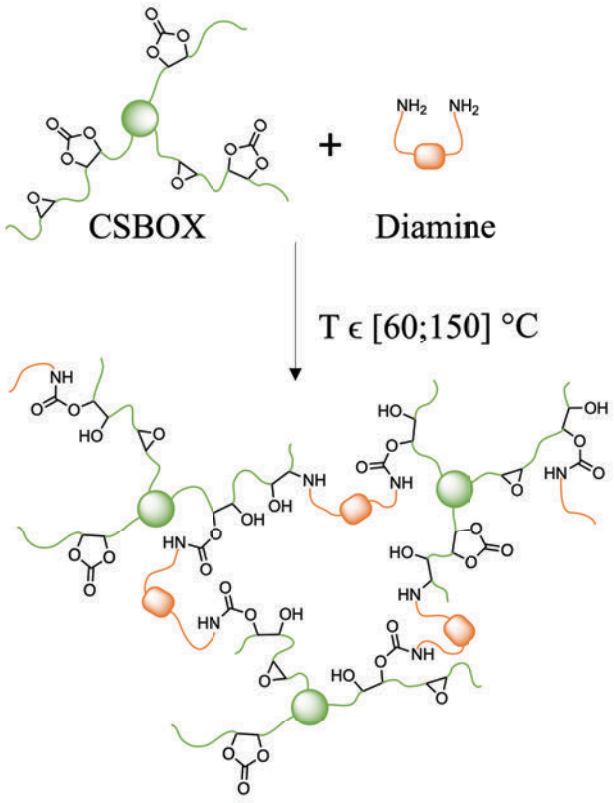

Figure 3 : Schematic representation of the crosslinking reaction of a partially carbonated epoxidized soybean oil (CSBOX) and a diamine

The crosslinking reaction with Priamine 1075 was first studied at 150 °C for 4 hours with various $[NH_2]$: [carbonate] : [epoxide] ratios *via* FTIR spectroscopy. Figure 4 represents the FTIR spectra collected as a function of time for $[NH_2]$ = [carbonate]. Clearly, the decrease of the intensity of the

characteristic absorption band of carbonate's carbonyl around 1808 cm^{-1} indicates that the aminolysis of the carbonate is effective. The slight decrease of the intensity of the absorption band of ester carbonyl at 1744 cm^{-1} confirms that the aminolysis of the triglyceride skeleton is another reaction that must be taken into account. The measurements of ester (α_{ester}) and carbonate ($\alpha_{carbonate}$) and the soluble fraction (w_{sol}) of the materials are reported in Table 1. Clearly, the results suggest that the optimal $[NH_2]$: [carbonate] : [epoxide] ratio is $[NH_2] = [carbonate] + \frac{[epoxide]}{2}$, as it maximizes the carbonate conversion while it minimizes the undesirable aminolysis of ester and the sol fraction. It suggests that the epoxides are involved in the crosslinking reaction of the system. However, it is impossible to quantitatively evaluate the extent of the epoxide aminolysis and thus to optimize the curing reaction.

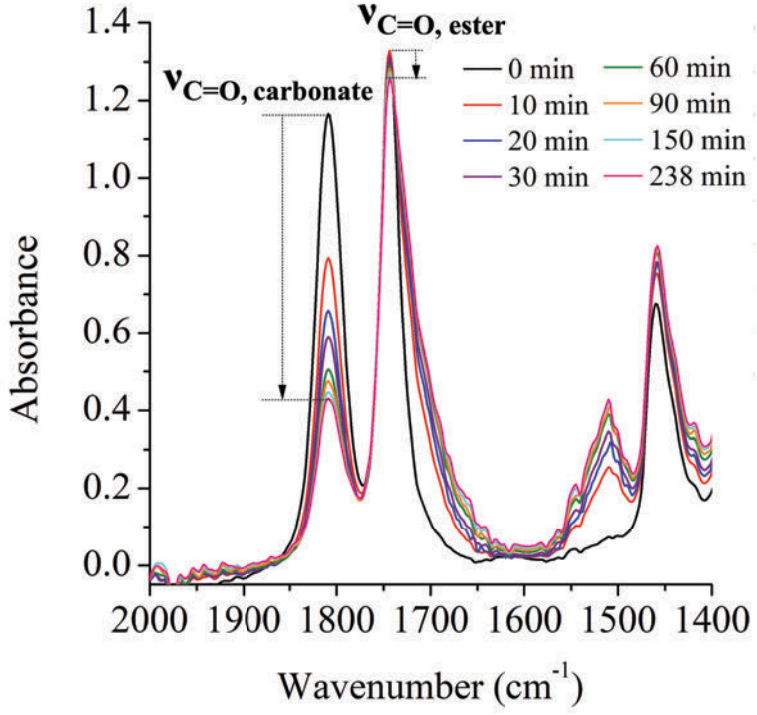

Figure 4 : Overlay of IR spectra collected during the 4-hour curing at 150 °C of the CSBO45-Priamine system considering $[NH_2]$ = [carbonate]

Table 1: Conversion of reactive functions during the 4-hour reaction at 150 °C between CSBO45 and Priamine 1045 and soluble fractions in toluene of the corresponding networks.

Ratio of reactive functions	$\alpha_{carbonate,\ f}$ (%)[a]	$\alpha_{ester,\ f}$ (%)[b]	w_{sol} (%)[c]
$[NH_2]$ = [carbonate]	64	6	51
$[NH_2]$ = [carbonate] + [epoxide]	88	41	50
$[NH_2] = [carbonate] + \frac{[epoxide]}{2}$	81	18	31

[a]Conversion of the carbonate functions and [b]conversion of the ester functions after 4 h of reaction at 150 °C as measured by FTIR spectroscopy. [c]The sol-fraction estimated by weighing the dried samples after swelling in toluene.

A first attempt to probe the involvement of the epoxides in the crosslinking reaction was made by considering the characteristic absorption band of epoxides around 840 cm^{-1} in infrared spectroscopy. However, as expected, the amplitude of the variation is too small to demonstrate whether they reacted with NH_2 or not. In order to confirm and better understand the reactivity of epoxides in this hybrid system, the crosslinking reaction was further investigated by Raman spectroscopy. In fact, this method has already been used to follow the synthesis of epoxides, the conversion of epoxides into carbonates or even the reaction of epoxides with amines.[42–46] Surprisingly, it has never been used to study the crosslinking reaction of ESBO with a diamine.

Figure 5 represents the Raman spectra of the various partially carbonated soybean oils, CSBOX with 45 % ≤ X ≤ 98 % (Figure 5a) as well as the evolution of the relative intensity, I, of the Raman band $\nu_{epoxide}$ investigated as a function of X (Figure 5b). Clearly, the intensity of the band $\nu_{epoxide}$ = 1267 cm^{-1} decreases linearly as X increases, suggesting that it is related to the vibration of the epoxide functions. This is consistent with the results reported by Parada Hernandez *et al.* and Gennen *et al*. showing that the Raman wavenumbers corresponding to the ring bending of epoxide are in the range of 1247 and 1260 cm^{-1}.[42,44] Thus, Raman spectroscopy is offering the possibility to quantitatively measure the conversion ratio of epoxide functions during the crosslinking reaction of ESBO and CSBOX with diamines. This was confirmed *via* an *in-situ* measurement of the Raman spectra during the crosslinking reaction of CSBO45 with Priamine 1075 at 120 °C ($[NH_2] = [carbonate]+\frac{[epoxide]}{2}$). Clearly, the intensity of the vibration band of epoxides decreases during the course of the reaction while the rest of the spectra remain unchanged (Figure S6), confirming that the epoxides are effectively reacting with the amines.

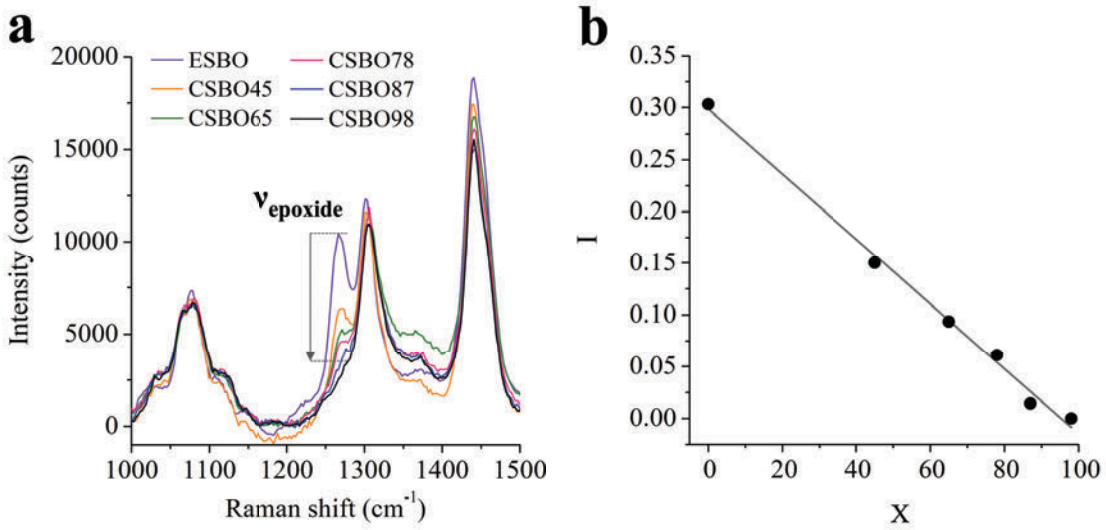

Figure 5: a) Stacking of ESBO and the different CSBOX Raman spectra with the decrease of the epoxides band at 1267 cm^{-1}; b) relative intensity of $\nu_{epoxide}$ = 1267 cm^{-1} as a function of the carbonation ratio X

With this new spectroscopic tool in hand, we studied the crosslinking reaction of CSBO45 with Priamine 1075 and 8DA at various temperatures T, 60 °C ≤ T ≤ 150 °C, during 4 h and with $[NH_2] = [carbonate] + \frac{[epoxide]}{2}$. For each temperature, the evolutions of $\alpha_{carbonate}$ and α_{ester} were measured through *in-situ* FTIR spectroscopy while the evolution of the epoxy conversion, $\alpha_{epoxide}$, was measured through *in-situ* Raman spectroscopy. The plots of the conversions as a function of time are represented in the ESI (Figure S7 to S13). The final conversions of ester ($\alpha_{ester, f}$), epoxy ($\alpha_{epoxy, f}$) and carbonate ($\alpha_{carbonate, f}$), *i.e.* the conversions measured after 4 h of reaction, are reported in Figure 6a for the various crosslinking temperatures, T.

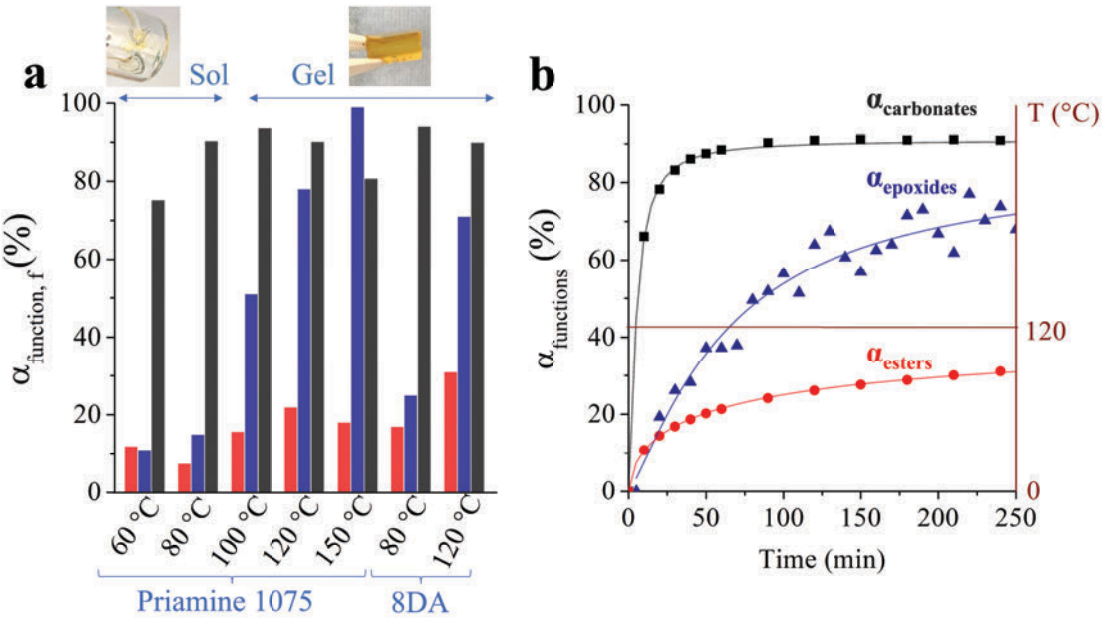

Figure 6: **(a)** Final conversions of carbonates (black), epoxides (blue) and esters (red) from CSBO45 mixed with either Priamine 1075 or 8DA after 4 h of reaction at temperature comprised between 60 and 150 °C; **(b)** detailed conversion curves as a function of time from the 4-hour reaction at 120 °C between CSBO45 + 8DA

For the crosslinking reaction with Priamine 1075, $\alpha_{carbonate, f}$ increases from 75 % to 92 % for T varying from 60 °C to 100 °C, indicating that the carbonate functions are effectively reacting with the amine even at rather low crosslinking temperature. On the other hand, $\alpha_{epoxy, f}$ increases from 15 % to 50 % on the same temperature range, revealing that the epoxy functions are much less reactive. In fact, for T = 60 °C and 80 °C, $\alpha_{epoxy, f} < 20$ %. For T varying from 100 °C to 120 °C, $\alpha_{carbonate, f}$ is slightly decreasing from 92 % to 80 % while $\alpha_{epoxy, f}$ surges from 50 % to nearly 100 %. The decrease of $\alpha_{carbonate, f}$ can be ascribed to the competition between the aminolysis of the carbonate and the epoxy functions. Moreover, a slight increase of $\alpha_{ester, f}$ indicates that the aminolysis of the esters might also play a role in the decrease of the availability of the amine functions, as previously described by other authors in the literature.[8,10,26,33,47,48] It is worth noting that, in this temperature range, additional side-reactions, including urea formation[11,49] or the reverse aminolysis of cyclic carbonate[47,50] can result in a decrease of $\alpha_{carbonate, f}$. The same observation is made for the crosslinking reaction with 8DA, although, at comparable crosslinking temperatures, 8DA, seemed to be more reactive than Priamine 1075 towards CSBO45, leading to higher values of $\alpha_{function}$ (Figure S12 and S13).

When considering the evolution of $\alpha_{function}$ as a function of time (Figure S7 to S13), it is clear that the kinetics of the aminolysis of epoxide are much slower than those of carbonates. Figure 6b represents the particular case of the crosslinking reaction of CSBO45 with 8DA at 120 °C. The plot of $\alpha_{carbonate}$ (black

square) indicates that the carbonate conversion reaches a plateau for $\alpha_{carbonate,\,f} \sim 90$ % in nearly t = 1 h, while the epoxy conversion (blue triangle) is of about 50 % at the same time. For both diamines and for all T values, the aminolysis kinetics of carbonate are faster than those of epoxide, even when $\alpha_{carbonate,\,f} < \alpha_{epoxide,\,f}$, confirming that the carbonates are much more reactive than the epoxides.

Once and for all, Raman spectroscopy provides direct and unambiguous evidence of the involvement of the epoxide in the crosslinking reaction of partially carbonated epoxidized soybean oil with diamines. More precisely, the dual-spectroscopic monitoring reveals two crosslinking regimes depending on T: (*i*) for T <100 °C, the *PHU regime* where the amines are essentially reacting with the carbonate functions to afford a polymer that is essentially a PHU prepolymer, (*ii*) for T ≥ 100 °C, the *hybrid regime* where both the carbonates and epoxides react with the amines and the resulting network is a hybrid thermosetting polymer, *i.e.* both a PHU and an epoxy-amine network.

Interestingly, the rheological properties of the polymer are drastically dependent on the crosslinking regime. For the crosslinking of CSBO45 with Priamine, in the *PHU regime*, the polymer is a viscous liquid (picture on the left, Figure 6a) that is fully soluble in toluene. After filtration of the solution over a PTFE filter (∅ = 45 μm), the SEC analysis of the solution indicates that it is mainly composed of CSBO45 (1260 g mol^{-1}), Priamine 1075 (480 g mol^{-1}) but also of oligomers with molar masses comprised between 2100 and 4600 g mol^{-1} (Figure S14). In the *hybrid regime*, the polymer is an elastic solid (picture on the right, Figure 6a), indicating the effective formation of a macroscopic gel. Thus, for the crosslinking of a partially carbonated ESBO with a carbonation ratio of about 50 %, it is mandatory to react both the carbonate and the epoxide functions to observe the formation of an elastic solid with a high gel content. While high conversions are reached for both carbonate and epoxide functions in this regime, the networks are not fully crosslinked, as evidenced by the swelling tests in toluene (Table 2): $w_s \sim 30$ %. These results are concordant with the literature as the soluble fractions are generally higher than 10 % for CSBO-based thermosets.[7,23,26,33] The high soluble fractions are usually the consequence of side reactions such as amidation (*i.e.* ester aminolysis), as evidenced by infrared monitoring (Figure 6). In our case, the intrinsic bulkiness of the Priamine contributes to further increase of the soluble fractions. Indeed, the resulting steric hindrance reduces the efficiency of the crosslinking reaction.

Table 2: Thermal properties and swelling data in toluene of the networks resulting from the crosslinking reactions of CSBO45 with Priamine 1075 and 8DA, ($[NH_2] = [\text{Carbonate}] + \frac{[\text{Epoxide}]}{2}$)

Diamine	Curing temperature (°C)	$T_{d,5\%}$ (°C)[a]	T_g (°C)[b]	Q (%)[c]	w_{sol} (%)[d]
Priamine 1075	60	281	-42	*Fully soluble*	
	80	278	-40	*Fully soluble*	

	100	278	-37	240	37
	120	282	-32	205	29
	150	289	-25	235	32
8DA	80	261	-6.5	180	53
	120	268	-4.0	100	22

[a]Temperature at 5 wt% loss determined by thermogravimetric analysis. [b]The glass transition temperature as measured by DSC. [c]The swelling ratio of the samples after immersion in toluene for at least 1 week (depending on the sample). [d]The sol-fraction estimated by weighing the samples dried after swelling in toluene.

For the crosslinking of CSBO45 with 8DA, in the *PHU regime*, the polymer behaves as an elastic gel. However, the swelling test in toluene indicates that the gel is barely crosslinked with a soluble fraction representing most of the weight of the material, w_{sol} ~ 53 wt%. In the *hybrid regime*, we obtained a gel with w_{sol} ~ 22 wt%. This is the lowest sol fraction observed in this study so far. The SEC analysis of the soluble fraction indicates that it is composed of unreacted CSBO45 and 8DA but also of oligomers with molar masses comprised between 3000 and 5000 g mol^{-1} (Figure S15). Again, these results indicate that it is mandatory to react both the epoxide and the carbonate functions to obtain an elastic solid with a high gel content. It also highlights the influence of the structure of the amine on the rheological properties of the polymers. With the short diamine 8DA, the polymer is as a gel both in the *PHU* and the *hybrid regime* while with Priamine, moving from one regime to the other results in the transition of the polymer from a viscous liquid to a gel.

These spectroscopic results are consistent with simple models such as the Carothers equation. Indeed, according to the literature, the typical functionality of epoxidized soybean oil is at least of $f_{epoxide}$ ~ 4, *i.e.* each triglyceride molecule contains, on average, 4 epoxides.[51] Thus, it is possible to estimate that, on average, the carbonate functionality of CSBO45, $f_{carbonate}$, is 0.45 × $f_{epoxide}$ ~ 1.8 carbonate functions. In these conditions, for the reaction of CSBO45 with a diamine (f_{NH2} = 2 and $[NH_2] = [\text{Carbonate}] + \frac{[\text{Epoxide}]}{2}$), if the carbonate functions solely react with the amines, then it is expected that the resulting polymer will be a viscous liquid. This is consistent with the properties of the polymers obtained by reacting CSBO45 with diamines in the *PHU regime*.

Rheometric investigation of the crosslinking reaction of CSBO45

The crosslinking reaction of CSBO45 with Priamine and 8DA, respectively, was further investigated through dynamic mechanical analysis in the multiwave mode using Fourier transform mechanical spectroscopy (FTMS). Figure 7a represents the evolution of the storage and the loss moduli, G' and G'' respectively (ω = 1 rad s^{-1}), as a function of time for the crosslinking reaction of CSBO45 with Priamine at T = 80 °C for 4 h, *i.e.* in the *PHU regime*. Clearly, G' < G'' for the whole experiment, indicating that

the polymer is not crosslinked at this temperature. Figure 7b represents the same experiment for T = 120 °C, *i.e.* in the *hybrid regime*. This time, the crossing point of G' and G'' (*i.e.* the gel point) is attained after t_{gel} ~ 95 min and G' reaches a plateau ~ 30 kPa, indicating the formation of a well crosslinked elastic gel. These results are consistent with the macroscopic aspects of the materials (Figure 6a) and the results of the swelling tests (Table 2). One can note that the gel points were determined thanks to the crossover of G' and G'' at the fundamental frequency (G' = G'' for ω = 1 rad s^{-1}, Tung and Dynes criterion).[52] By using the G' and G'' values collected for the harmonic frequencies (ω = 3, 6, 10, 30, 60 and 100 rad s^{-1}), t_{gel} was also determined according to the Winter and Chambon criterion, the most accurate one (tan(δ) = constant for all the frequencies, see Figure S16).[41] The results indicate that both criteria provide a similar value of t_{gel}. Thus, for the sake of simplicity, the simpler Tung and Dynes criterion is used in the rest of the discussion.

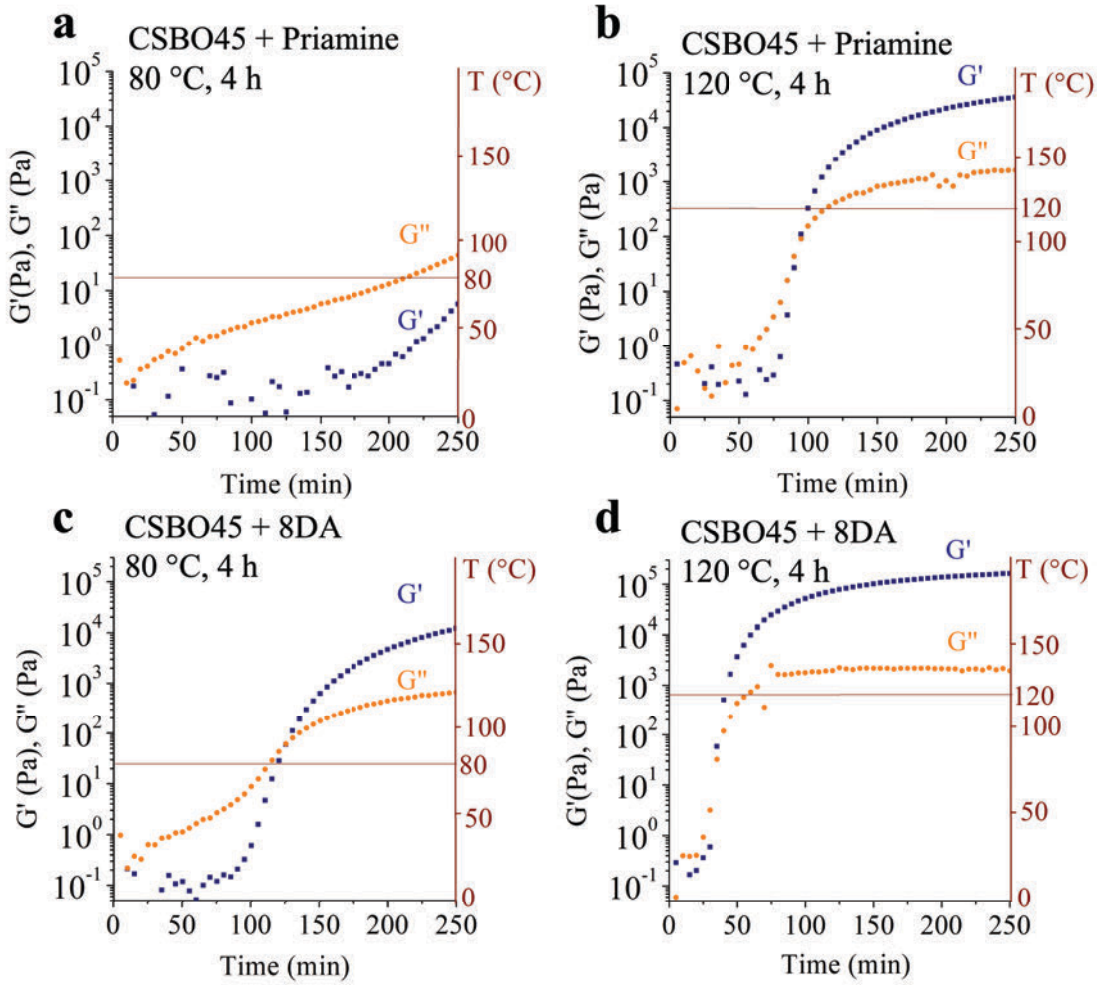

Figure 7: Rheological monitoring of the 4-hour curing of the system CSBO45-Priamine 1075 at (a) 80 °C and (b) 120 °C and the system CSBO45-8DA at (c) 80 °C and (d) 120 °C

Figure 7c and Figure 7d represent the same experiments for the crosslinking reaction of CSBO45 with 8DA. In the *PHU regime* (T = 80 °C, Figure 7c), t_{gel} ~ 125 min and G' ~ 10 kPa after 4 h. In the *hybrid regime* (T = 120 °C, Figure 7d), t_{gel} ~ 35 min and G' ~ 150 kPa after 4 h. Again, these results are consistent with those of the swelling tests (Table 2). Indeed, in the *PHU regime*, the material is a lightly crosslinked gel with a low storage modulus, in accordance with the predominance of the sol fraction (w_{sol} ~ 53 wt%). In the *hybrid regime*, the material is a well crosslinked gel with a high storage modulus, which is correlating well with the substantial decrease of w_{sol} ~ 22 wt%.

The rheometric measurements confirm that partially carbonated ESBO, CSBO45, can be crosslinked *via* a two-step process. During the first step (*PHU regime*) the carbonate functions react to afford a prepolymer that is essentially a PHU, in the form of a viscous liquid or a lightly crosslinked elastic gel. During the second step (*hybrid regime*), further increase of the crosslinking temperature initiates the epoxy-amine reaction to afford a hybrid thermosetting polymer.

The completion of the crosslinking reaction in the *hybrid regime* is also confirmed by measuring the glass transition temperatures (T_g) of the polymers by dynamic scanning calorimetry (DSC – Table 2 and Figure S17-S18). For the crosslinking of CSBO45 with Priamine, the T_g increases significantly from ~ -40 °C for T < 100 °C, to ~ -25 °C for T = 150 °C. For the crosslinking of CSBO45 with 8DA, only a slight increase of the T_g from ~ -6.5 °C for T = 80 °C, to ~ -4 °C for T = 120 °C is measured. These results illustrate the influence of the structure of the amine on the T_g of the polymer. Indeed, due to the shorter backbone of 8DA as compared to Priamine, the crosslink density of the 8DA-based polymers is intrinsically higher than those of the Priamine-based polymers, and so are the T_g's.

Crosslinking reactions of ESBO with Priamine

The results obtained in Raman spectroscopy demonstrate that the reaction of the epoxy functions of CSBO45 is effective in the *hybrid regime* and that it is crucial to observe the formation of a crosslinked network. This is a rather counterintuitive conclusion given that, according to several reports in the literature, it is not possible to crosslink a ESBO-diamine mixture in such conditions, even though the same reaction should be operative in this system.[30,33] Our findings incited us to gain more insight into the ESBO-diamine system. First, it is interesting to note that, according to the Carothers model, the sol-gel transition is expected for a ESBO-diamine mixture, providing that the epoxy-amine reaction is effective. Indeed, by considering that $f_{epoxide}$ ~ 4 for ESBO, then, according to the Carother's equation, for $[NH_2] = \frac{[\text{epoxide}]}{2}$, the gel point of the crosslinking reaction of ESBO with a diamine (f_{NH} ~ 4) should be observed for epoxy conversions as low as $\alpha_{epoxy} = 2/f_{av} \times 100 = 50$ %, where f_{av} is the average functionality of the system ($f_{av} = f_{epoxide} + f_{NH} / 2 = 4$).

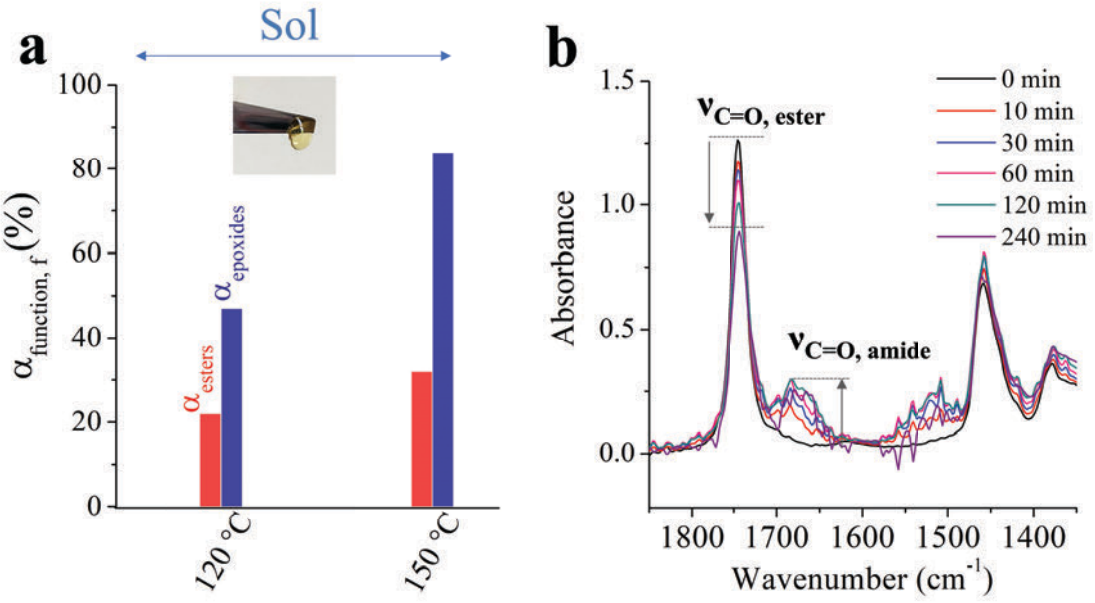

Figure 8 : **(a)** Final conversions of epoxides (blue) and esters (red) from ESBO mixed with Priamine 1075 after 4 h of reaction at either 120 or 150 °C; **(b)** Overlay of IR spectra acquired during the *in-situ* monitoring of the reaction at 150 °C involving ESBO and Priamine, 2100-1300 cm^{-1} zone

Here, we used FTIR and Raman spectroscopies, combined with rheometry, to investigate the crosslinking reaction of ESBO with Priamine ($[NH_2] = \frac{[Epoxide]}{2}$), for T = 120 °C and 150 °C, *i.e.* T values in the temperature range corresponding to the *hybrid regime* of CSBO45. Figure 8a represents the final conversion of esters and epoxides, $\alpha_{ester, f}$ and $\alpha_{epoxy, f}$, after 4 h of reaction, measured *via* FTIR and Raman spectroscopy respectively, and the detailed conversion curves are represented in Figure S19 and S20. For T = 120 °C and 150 °C, $\alpha_{epoxy, f}$ = 48 % and 80 % respectively and for both temperatures, the final polymer is a viscous liquid that is fully soluble in toluene (see picture in Figure 8a). According to the Carothers equation, T = 150 °C should be sufficient to observe the formation of a gel. The soluble fraction was analyzed by SEC (Figure S21) which revealed the presence of oligomers with molar masses $\leq$ 4000 g mol^{-1}. Rheometry also revealed that, for both temperatures, G' < G'' throughout the whole experiment (Figure S19 and S20). One can note that viscous liquids are also obtained in the same conditions when the reaction between ESBO and 8DA is studied, confirming that ESBO cannot be crosslinked by regular alkyl diamines. Thanks to the novelty of our experimental approach with the use of Raman spectroscopy, we can confirm that the epoxide-amine reaction is well effective though. Thus, the absence of the sol-gel transition indicates the existence of side reactions that preclude the formation of a crosslinked network.

The aminolysis of the triglyceride skeleton of ESBO is one of these side reactions. It results in a degradation of the epoxidized oil and thus in a decrease of the average functionality of the system, f_{av}. This side reaction is clearly observed during the *in-situ* infrared monitoring (Figure 8b and Figure S19, S20). In fact, for T = 150 °C, $\alpha_{ester,f} \sim 30$ %.

Due to the very low molar masses measured by SEC, we suspect that intramolecular reactions, also called cyclization, might impede the formation of a crosslinked network as well. In ESBO based system, we believe that the probability for a secondary amine NH, resulting from the reaction between an amino and an epoxide function, to react with another epoxide group from the same triglyceride skeleton is high, as described in Figure 9. This can be considered as an intramolecular reaction that does not contribute to the crosslinking reaction of the system.

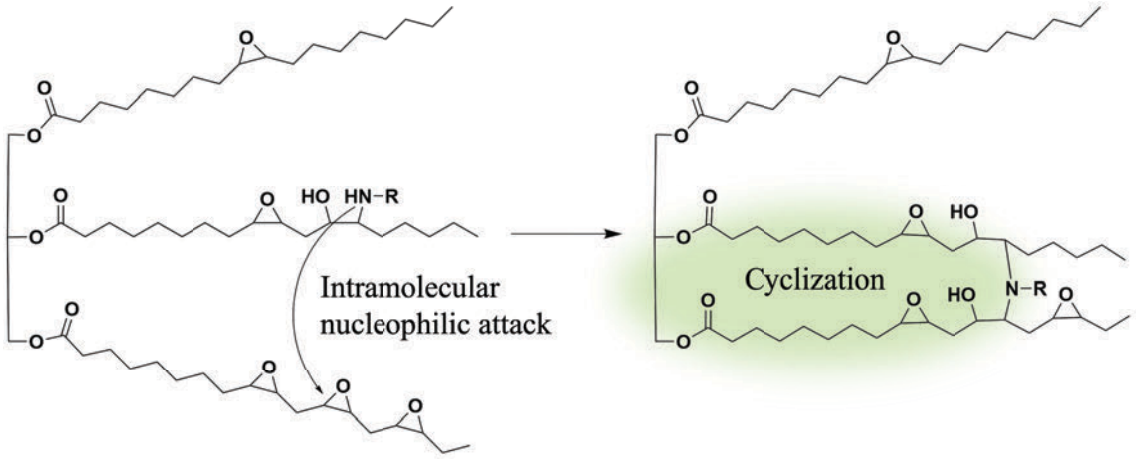

Figure 9 : Intramolecular reaction between an amino and an epoxide group during the curing of an ESBO-based polymer

Based on this new insight of the ESBO-diamine system, the effective gelation of the CSBOX-diamine system seems to be related to the much higher reactivity of the carbonate functions *vs* the esters of the triglyceride skeleton, with the diamine. Indeed, according to the spectroscopic data reported in the present study, the reactivity of the various functional groups of CSBOX with diamines are ranged as follow: carbonate > epoxide > ester. Thus, in the CSBOX-diamine system, the overall competition between the aminolysis of the carbonates, the epoxides and the esters result in a significant and beneficial decrease of the ester aminolysis rate. Additionally, the 1:1 stoichiometry of the carbonate *vs* NH_2 reaction probably contributes to a decrease of the occurrence of cyclization reactions.

Interestingly, the present study demonstrates that the partial carbonation of ESBO is sufficient to obtain a crosslinkable system. Moreover, the results suggest that the reactions of the various functions can be

orchestrated by controlling the crosslinking temperature. It paves the way towards the design of new thermolatent systems.

Thermolatent systems based on CSBOX

The two crosslinking regimes of CSBOX could be valorised to imagine new stepwise curing sequences for soybean oil-based thermosets. For instance, the increase of the viscosity during the *PHU regime* could be used to improve the processability of the system before the sol-gel transition in the *hybrid regime*. Moreover, the optimization of the curing sequence could help improve the crosslinking degree of the final thermosetting polymers, and, in return, their thermo-mechanical properties. This was illustrated by testing different curing sequences for the crosslinking reaction of CSBO45 with the Priamine 1075 and 8DA. The primary objective is to discriminate, as a function of the temperature, the carbonate-amine and epoxy-amine reactions and to limit the extent of the side reactions. To do so, several experiments were carried out involving a two-step curing process: (*i*) *step 1*: curing at T_1 (°C) for t_1 hours, (*ii*) *step 2*: curing at T_2 (°C) for t_2 hours. The crosslinking reactions were monitored by FTIR and Raman spectroscopy as well as rheology. Comparative experiments involving ESBO instead of CSBO45 were also carried out. The curing temperatures of each step were chosen based on the knowledge of the temperature range of the *PHU* and the *hybrid regimes*: (*i*) T_1 = 80 °C, (*ii*) T_2 = 120 °C.

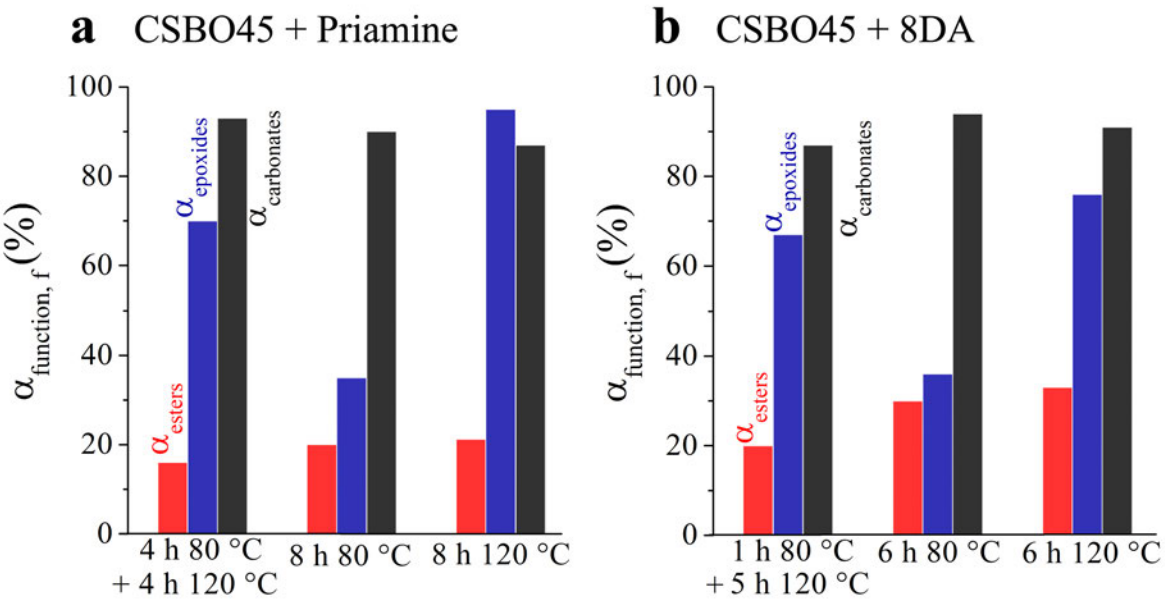

Figure 10 : Final conversion of carbonate functions (black), epoxide functions (blue) and ester functions (red) for the systems CSBO45 mixed with a) Priamine 1075 and b) 8DA after a two-step or one-step curing sequence

In the case of the CSBO45-Priamine system, the first step at T_1 = 80 °C was conducted for t_1 = 4 h as it was the time needed to reach a plateau for the conversion of the carbonate functions at this temperature. The second step at T_2 = 120 °C was conducted for t_2 = 4 h as well (see Figure S22 for detailed conversion ratio). The final conversions, $\alpha_{ester,\,f}$, $\alpha_{epoxide,\,f}$ and $\alpha_{carbonate,\,f}$ at the end of the curing sequence, are reported in the diagram of Figure 10a. This two-step process is efficient as the carbonate conversion ratio reached $\alpha_{carbonate}$ = 90 % at the end of the first step and the epoxide conversion $\alpha_{epoxide}$ = 70 % after the second step. According to the rheological monitoring (Figure S22), the first step corresponds to a gradual increase of the moduli G' and G'' with no sign of gelation. As expected, it can be considered as a prepolymerization step, which could include the shaping process of the material. The sol-gel transition is observed shortly after the beginning of the second step: t_{gel} = 4.8 h (Table 3). The resulting network was swollen in toluene indicating a swelling ratio of Q = 202 % and a sol fraction of w_{sol} = 28 %. The thermal properties were characterized by TGA ($T_{d5\%}$ = 290 °C) and DSC (T_g = -28 °C). All the data are collected in Table 3 (see Figure S23 and S24 for detailed analyses). To illustrate the potential benefits of this two-step curing sequence, it was compared to one-step curing sequences at 80 °C (t_1 = 8 h, t_2 = 0, Figure S25) and at 120 °C (t_1 = 0, t_2 = 8 h, Figure S26). The final conversions are reported in Figure 10a as well and the data related to the thermo-mechanical properties and the swelling test of the resulting crosslinked networks in toluene are reported in Table 3. Clearly, the large increase of w_{sol} in the case of the one-step curing sequence at 80 °C (w_{sol} = 49 %) indicates that a curing step at 120 °C is mandatory to obtain a fully crosslinked network. Once again, this result can be explained by the large increase of the epoxy conversion, $\alpha_{epoxide}$, from ~ 35 % for the one-step curing sequence at 80 °C to ~ 70 % for the 2-step curing sequence (Figure 10a). The comparison of the one-step curing at 120 °C *vs* the two-step sequences indicates that the properties of the resulting networks are very similar. However, the gel time is much shorter in the case of the one-step curing sequence (t_{gel} = 1.6 h), leaving a tighter time window for handling and processing the material. Thus, the two-step approach is a convenient way to increase the delay between the beginning of the curing process and the sol-gel transition, *i.e.* the latency, while gradually increasing the viscosity.[53]

Table 3 : Curing parameters, gel time, thermal properties and swelling data for the networks resulting from the crosslinking reactions of CSBO45 with Priamine 1075 and 8DA ($[NH_2] = [carbonate]+\frac{[epoxide]}{2}$)

Diamine	Curing sequence		t_{gel} (h)[a]	$T_{d,5\%}$ (°C)[b]	T_g (°C)[c]	Q (%)[d]	w_{sol} (%)[e]
	t_1 (h), T_1 = 80 °C	t_2 (h), T_2 = 120 °C					
Priamine 1075	4	4	4.8	290	-28	202	28
	8	0	5.5	282	-34	364	49
	0	8	1.6	283	-27	195	23
8DA	1	5	1.3	270	-4	77	14
	6	0	2.1	264	-7	140	36

0	6	0.6	269	-1	97	19

[a]The gel time was measured by dynamic mechanical analysis in rheology. [b]Temperature at 5 wt % loss determined by thermogravimetric analysis. [c]The glass transition temperature as measured by DSC. [d]The swelling ratio of the samples after immersion in toluene for at least 1 week (depending on the sample). [e]The sol-fraction estimated by weighing the dried samples after swelling in toluene.

In the case of the CSBO45-8DA system, the first step at T_1 = 80 °C was conducted for t_1 = 1 h and the second step at T_2 = 120 °C was maintained for t_2 = 5 h (see Figure S27 for detailed conversion ratio). Once again, the two-step curing sequence was compared to one-step curing sequences at 80 °C (t_1 = 6 h, t_2 = 0, Figure S28) and at 120 °C (t_1 = 0, t_2 = 6 h, Figure S29). The final conversions of the reactive functions are reported in Figure 10b and the data related to the thermo-mechanical properties and the swelling test of the resulting crosslinked networks in toluene are reported in Table 3 (see Figure S30 and S31 for detailed analyses). Similarly to the CSBO45-Priamine system, the two-step curing sequence allows an efficient discrimination of the carbonate and the epoxide aminolysis ($\alpha_{carbonate}$ ~ 80 % at the end of the first step followed by a surge of the epoxide conversion during the second step from $\alpha_{epoxide}$ ~ 10 % to ~ 70 %, see Figure 10b and Figure S27) and the sol-gel transition is observed shortly after the beginning of the second step, t_{gel} = 1.3 h. The sol fraction w_{sol} = 14 % indicates that the crosslinking reaction is very efficient. For the one-step curing process at 80 °C, the large increase of the sol-fraction w_{sol} = 36 % indicates that the crosslinking is much less efficient. Once again this is correlated to the very low conversion of the epoxides, $\alpha_{epoxide, f}$ ~ 35 %, at the end of the curing sequence (see Figure 10b and S28). The one-step curing process at 120 °C provides a material with very similar properties to the one of the two-step sequence. A slight decrease of w_{sol} in the latter case suggests that the two-step curing sequence might be beneficial to limit the extent of the side-reactions. This is further confirmed by considering the final conversion of the ester function, $\alpha_{ester, f}$: $\alpha_{ester, f}$ ~ 20% in the case of the two-step approach while $\alpha_{ester, f}$ ~ 30% for the one-step curing sequences. It is worth noting that in all cases, the sol-gel transition is observed for lower values of t_{gel} as compared to the CSBO45-priamine 1075 system, with $t_{gel} \leq 2$ h for the three curing sequences, revealing a much shorter thermal latency for CSBO45-8DA.

As a comparison, the same curing sequences were applied to the ESBO-Priamine 1075 and the ESBO-8DA systems (see Figure S32 and S33 for detailed conversion ratios). In both cases, there was no evidence of the sol-gel transition in rheology and the reaction products were fully soluble in toluene, as previously observed for the one-step curing process of the ESBO-Priamine 1075 system at 120 °C and 150 °C (see Figure 8). SEC analyses (Figure S34) revealed the presence of oligomers with molar masses < 4000 g mol^{-1}, whose formation could be mainly explained by the degradation of the triglyceride skeleton attested by the aminolysis of a large amount of ester functions (α_{ester} ~ 50 %, Figure S32 and S33). Those experiments confirm the real advantage to work with a hybrid system, comprising both carbonate and epoxide functions.

Conclusions

The present study sheds a new light on the crosslinking reaction of epoxidized and carbonated soybean oil with diamines. In particular, the dual-spectroscopic monitoring provides a comprehensive understanding of the reactivity of carbonates, epoxides and esters in a partially carbonated soybean oil, such as CSBO45. Thus, the reactivity of epoxides was undeniably demonstrated and quantitatively evaluated through Raman spectroscopy, allowing the comparison with those of carbonates and esters (measured by IR spectroscopy). The spectroscopic data indicate that the reactivities are ranged as follow: carbonate > epoxide > ester. Interestingly, the investigation of the crosslinking reaction at various temperatures indicates that two regimes can be discriminated: (i) for $T < 100$ °C, the *PHU regime*, during which most of the carbonate functions of CSBO45 react while the epoxy functions are essentially unreactive, (ii) for $T \geq 100$ °C, a *hybrid regime*, during which both the carbonate and the epoxide functions react to completion. Moreover, the investigation of the crosslinking reaction through rheometric measurements indicates that the sol-gel transition is only possible during the *hybrid regime*, *i.e.* once the epoxides are involved in the crosslinking reaction.

Another important lesson of the present study is the confirmation that it is indeed very difficult to crosslink neat ESBO through epoxy-amine chemistry. The unprecedented results provided by the dual-spectroscopic monitoring indicate that this is mostly due to the competition between the epoxy-amine and the ester-amine reactions. Indeed, in the *hybrid regime*, the rate of the ester-amine reaction is not negligeable anymore so that the triglyceride skeleton is degraded making the sol-gel transition impossible. Interestingly, we demonstrate that the partial carbonation of ESBO is sufficient to obtain a crosslinkable system. In the presence of the highly reactive carbonate functions, the overall competition between the aminolysis of the carbonates, the epoxides and the esters result in a significant and beneficial decrease of the ester aminolysis rate. In the end, with this new understanding of the reactivity, it is possible to orchestrate the reactions of the various functions in order to optimize the crosslinking degree of the resulting thermosets and their thermo-mechanical properties.

Eventually, this study paves the way towards the design of new biobased thermolatent crosslinkable formulations. The two crosslinking regimes were valorised to imagine new curing sequences for soybean oil-based thermosets. The rheological investigations reveal that a first step at 80 °C can lead to an increase of the viscosity of the systems and act as a pre-polymerization step, offering plenty of time to shape the polymer. A second step at 120 °C fosters the reaction and results in a fast sol-gel transition to set the polymer in its final shape. Interestingly, the two-step curing sequence appeared as a good technique to limit the side reaction of ester aminolysis. It helps improve the crosslinking degree of the final thermosetting polymers.

Associated content

Electronic Supporting Information ESI

Characterization methods, additional ^{1}H NMR spectra of ESBO and partially carbonated ESBO, example of IR and Raman spectra recorded during the in-situ monitoring of CSBO45 crosslinking, conversion curves of carbonates, epoxides and esters, respectively, as a function of time as well as rheological monitoring for the different curing conditions, SEC traces of soluble fractions and monomers and DSC traces of polymers.

Author information

Corresponding Authors

Thomas Vidil − Univ. Bordeaux, CNRS, Bordeaux INP, LCPO, 33600 Pessac, France; orcid.org/0000-0002-6218-3418; Email: thomas.vidil@enscbp.fr

Henri Cramail − Univ. Bordeaux, CNRS, Bordeaux INP, LCPO, 33600 Pessac, France; orcid.org/0000-0001-9798-6352; Email: cramail@enscbp.fr

Authors

Péroline Helbling − Univ. Bordeaux, CNRS, Bordeaux INP, LCPO, 33600 Pessac, France ; Saint-Gobain Recherche Paris, 93300 Aubervilliers, France

Fabien Hermant − Saint-Gobain Research Paris, 93300 Aubervilliers, France

Morgane Petit − Saint-Gobain Research Paris, 93300 Aubervilliers, France

Thierry Tassaing − Univ. Bordeaux, CNRS, Bordeaux INP, ISM, 33405 Talence, France

Acknowledgments

The authors gratefully thank Saint-Gobain Recherche Paris for the financial support. The authors genuinely thank ITERG for providing the ESBO, Paul Marque (Univ. Bordeaux, CNRS, Bordeaux INP, LCPO) as well as Cédric Le Coz (Univ. Bordeaux, CNRS, Bordeaux INP, LCPO) for collaborating respectively on infrared spectroscopy and rheological experiments and enabling this study.

References

1 H. W. Engels, H. G. Pirkl, R. Albers, R. W. Albach, J. Krause, A. Hoffmann, H. Casselmann and J. Dormish, Polyurethanes: Versatile materials and sustainable problem solvers for today's challenges, *Angew. Chemie - Int. Ed.*, 2013, **52**, 9422–9441.

2 PlasticsEurope, *Plastics - The Facts 2021*, 2021.

3 EUROPEAN PARLIAMENT, COMMISSION REGULATION (EU) 2020/1149 amending Annex XVII to Regulation (EC) No 1907/2006 of the European Parliament and of the Council concerning the Registration, Evaluation, Authorisation and Restriction of Chemicals (REACH) as regards diisocyanates, *Off. J. Eur. Union*, 2020, **2020/1149**, 24–29.

4 L. Maisonneuve, O. Lamarzelle, E. Rix, E. Grau and H. Cramail, Isocyanate-Free Routes to Polyurethanes and Poly(hydroxy Urethane)s, *Chem. Rev.*, 2015, **115**, 12407–12439.

5 A. Cornille, R. Auvergne, O. Figovsky, B. Boutevin and S. Caillol, A perspective approach to sustainable routes for non-isocyanate polyurethanes, *Eur. Polym. J.*, 2017, **87**, 535–552.

6 A. Gomez-Lopez, F. Elizalde, I. Calvo and H. Sardon, Trends in non-isocyanate polyurethane (NIPU) development, *Chem. Commun.*, 2021, **57**, 12254–12265.

7 B. Tamami, S. Sohn and G. L. Wilkes, Incorporation of Carbon Dioxide into Soybean Oil and Subsequent Preparation and Studies of Nonisocyanate Polyurethane Networks, *J. Appl. Polym. Sci.*, 2004, **92**, 883–891.

8 I. Javni, D. P. Hong and Z. S. Petrovič, Polyurethanes from soybean oil, aromatic and cycloaliphatic diamines by nonisocyanate route, *J. Appl. Polym. Sci.*, 2013, **128**, 566–571.

9 S. Panchireddy, B. Grignard, J. M. Thomassin, C. Jerome and C. Detrembleur, Bio-based poly(hydroxyurethane) glues for metal substrates, *Polym. Chem.*, 2018, **9**, 2650–2659.

10 S. Doley and S. K. Dolui, Solvent and catalyst-free synthesis of sunflower oil based polyurethane through non-isocyanate route and its coatings properties, *Eur. Polym. J.*, 2018, **102**, 161–168.

11 O. Lamarzelle, P. L. Durand, A. L. Wirotius, G. Chollet, E. Grau and H. Cramail, Activated lipidic cyclic carbonates for non-isocyanate polyurethane synthesis, *Polym. Chem.*, 2016, **7**, 1439–1451.

12 C. Carré, L. Bonnet and L. Avérous, Solvent- and catalyst-free synthesis of fully biobased nonisocyanate polyurethanes with different macromolecular architectures, *RSC Adv.*, 2015, **5**, 100390–100400.

13 B. Bizet, E. Grau, H. Cramail and J. M. Asua, Volatile Organic Compound-Free Synthesis of Waterborne Poly(hydroxy urethane)-(Meth)acrylic Hybrids by Miniemulsion Polymerization, *ACS Appl. Polym. Mater.*, 2020, **2**, 4016–4025.

14 M. Fleischer, H. Blattmann and R. Mülhaupt, Glycerol-, pentaerythritol- and trimethylolpropane-based polyurethanes and their cellulose carbonate composites prepared via the non-isocyanate route with catalytic carbon dioxide fixation, *Green Chem.*, 2013, **15**, 934–942.

15 F. Magliozzi, G. Chollet, E. Grau and H. Cramail, Benefit of the Reactive Extrusion in the Course

of Polyhydroxyurethanes Synthesis by Aminolysis of Cyclic Carbonates, *ACS Sustain. Chem. Eng.*, 2019, **7**, 17282–17292.

16 F. Magliozzi, A. Scali, G. Chollet, E. Grau and H. Cramail, Enantioselective Crystallization of Diglycerol Dicarbonate: Impact of the Microstructure on Polyhydroxyurethane Properties, *Macromol. Rapid Commun.*, 2021, **42**, 1–9.

17 S. Schmidt, N. E. Göppert, B. Bruchmann and R. Mülhaupt, Liquid sorbitol ether carbonate as intermediate for rigid and segmented non-isocyanate polyhydroxyurethane thermosets, *Eur. Polym. J.*, 2017, **94**, 136–142.

18 P. K. Dannecker and M. A. R. Meier, Facile and Sustainable Synthesis of Erythritol bis(carbonate), a Valuable Monomer for Non-Isocyanate Polyurethanes (NIPUs), *Sci. Rep.*, 2019, **9**, 1–6.

19 X. C. Xuedong Xi, Antonio Pizzi, Christine Gerardin, Hong Lei, Siham Amirou, Preparation and Evaluation of Glucose Based Non-Isocyanate Polyurethane Self-Blowing Rigid Foams, *Polymers*, 2019, **11**, 1802.

20 V. Salvado, M. Dolatkhani, E. Grau, T. Vidil and H. Cramail, Sequence-controlled polyhydroxyurethanes with tunable regioregularity obtained from biobased vicinal bis-cyclic carbonates, *Macromolecules*, 2022, **55**, 7249–7265.

21 V. Schimpf, B. S. Ritter, P. Weis, K. Parison and R. Mülhaupt, High Purity Limonene Dicarbonate as Versatile Building Block for Sustainable Non-Isocyanate Polyhydroxyurethane Thermosets and Thermoplastics, *Macromolecules*, 2017, **50**, 944–955.

22 K. A. Maltby, M. Hutchby, P. Plucinski, M. G. Davidson and U. Hintermair, Selective Catalytic Synthesis of 1,2- and 8,9-Cyclic Limonene Carbonates as Versatile Building Blocks for Novel Hydroxyurethanes, *Chem. - A Eur. J.*, 2020, **26**, 7405–7415.

23 X. Liu, X. Yang, S. Wang, S. Wang, Z. Wang, S. Liu, X. Xu, H. Liu and Z. Song, Fully Bio-Based Polyhydroxyurethanes with a Dynamic Network from a Terpene Derivative and Cyclic Carbonate Functional Soybean Oil, *ACS Sustain. Chem. Eng.*, 2021, **9**, 4175–4184.

24 A. Lee and Y. Deng, Green polyurethane from lignin and soybean oil through non-isocyanate reactions, *Eur. Polym. J.*, 2015, **63**, 67–73.

25 B. Grignard, J. M. Thomassin, S. Gennen, L. Poussard, L. Bonnaud, J. M. Raquez, P. Dubois, M. P. Tran, C. B. Park, C. Jerome and C. Detrembleur, CO_2-blown microcellular non-isocyanate polyurethane (NIPU) foams: From bio- and CO_2-sourced monomers to potentially thermal insulating materials, *Green Chem.*, 2016, **18**, 2206–2215.

26 M. Bähr and R. Mülhaupt, Linseed and soybean oil-based polyurethanes prepared via the non-isocyanate route and catalytic carbon dioxide conversion, *Green Chem.*, 2012, **14**, 483–489.

27 C. Mokhtari, F. Malek, A. Manseri, S. Caillol and C. Negrell, Reactive jojoba and castor oils-based cyclic carbonates for biobased polyhydroxyurethanes, *Eur. Polym. J.*, 2019, **113**, 18–28.

28 K. M. Doll and S. Z. Erhan, The improved synthesis of carbonated soybean oil using supercritical carbon dioxide at a reduced reaction time, *Green Chem.*, 2005, **7**, 849–854.

29 M. Alves, B. Grignard, S. Gennen, C. Detrembleur, C. Jerome and T. Tassaing, Organocatalytic synthesis of bio-based cyclic carbonates from CO_2 and vegetable oils, *RSC Adv.*, 2015, **5**, 53629–53636.

30 L. Poussard, J. Mariage, B. Grignard, C. Detrembleur, C. Jérome, C. Calberg, B. Heinrichs, J. De Winter, P. Gerbaux, J. M. Raquez, L. Bonnaud and P. Dubois, Non-Isocyanate Polyurethanes from Carbonated Soybean Oil Using Monomeric or Oligomeric Diamines to Achieve Thermosets or Thermoplastics, *Macromolecules*, 2016, **49**, 2162–2171.

31 W. Y. Perez-Sena, K. Eränen, N. Kumar, L. Estel, S. Leveneur and T. Salmi, New insights into the cocatalyst-free carbonation of vegetable oil derivatives using heterogeneous catalysts, *J. CO_2 Util.*, 2022, **57**, 101879.

32 A. Centeno-Pedrazo, J. Perez-Arce, S. Prieto-Fernandez, Z. Freixa and E. J. Garcia-Suarez, Phosphonium-based ionic liquids: Economic and efficient catalysts for the solvent-free cycloaddition of CO_2 to epoxidized soybean vegetable oil to obtain potential bio-based polymers precursors, *Mol. Catal.*, 2021, **515**, 111889.

33 S. Javni, I., Hong, D. P., Petrovic, Z., Soy-Based Polyurethanes by Nonisocyanate Route, *J. Appl. Polym. Sci.*, 2008, **108**, 3867–3875.

34 Y. Y. Liu, J. He, Y. D. Li, X. L. Zhao and J. B. Zeng, Biobased, reprocessable and weldable epoxy vitrimers from epoxidized soybean oil, *Ind. Crops Prod.*, 2020, **153**, 112576.

35 X. Yang, S. Wang, X. Liu, Z. Huang, X. Huang, X. Xu, H. Liu, D. Wang and S. Shang, Preparation of non-isocyanate polyurethanes from epoxy soybean oil: Dual dynamic networks to realize self-healing and reprocessing under mild conditions, *Green Chem.*, 2021, **23**, 6349–6355.

36 Z. S. Liu, S. Z. Erhan, J. Xu and P. D. Calvert, Development of soybean oil-based composites by solid freeform fabrication method: Epoxidized soybean oil with bis or polyalkyleneamine curing agents system, *J. Appl. Polym. Sci.*, 2002, **85**, 2100–2107.

37 Y. D. Li, X. Y. Jian, J. Zhu, A. K. Du and J. B. Zeng, Fully biobased and high performance epoxy thermosets from epoxidized soybean oil and diamino terminated polyamide 1010 oligomers,

Polym. Test., 2018, **72**, 140–146.

38 C. F. Frias, A. C. Serra, A. Ramalho, J. F. J. Coelho and A. C. Fonseca, Preparation of fully biobased epoxy resins from soybean oil based amine hardeners, *Ind. Crops Prod.*, 2017, **109**, 434–444.

39 US Pat., 0 208 967, 2012.

40 O. Figovsky, L. Shapovalov, O. Birukova and A. Leykin, Modification of epoxy adhesives by hydroxyurethane components on the basis of renewable raw materials, *Polym. Sci. - Ser. D*, 2013, **6**, 271–274.

41 T. Vidil, M. Cloître and F. Tournilhac, Control of Gelation and Network Properties of Cationically Copolymerized Mono- and Diglycidyl Ethers, *Macromolecules*, 2018, **51**, 5121–5137.

42 N. L. Parada Hernandez, A. J. Bonon, J. O. Bahú, M. I. R. Barbosa, M. R. Wolf Maciel and R. M. Filho, Epoxy monomers obtained from castor oil using a toxicity-free catalytic system, *J. Mol. Catal. A Chem.*, 2017, **426**, 550–556.

43 I. Nykulyshyn, Z. Pikh, L. Shevchuk and S. Melnyk, Examining the epoxidation process of soybean oil by peracetic acid, *Eastern-European J. Enterp. Technol.*, 2017, **3**, 21–28.

44 S. Gennen, M. Alves, R. Méreau, T. Tassaing, B. Gilbert, C. Detrembleur, C. Jerome and B. Grignard, Fluorinated alcohols as activators for the solvent-free chemical fixation of carbon dioxide into epoxides, *ChemSusChem*, 2015, **8**, 1845–1849.

45 R. Hardis, J. L. P. Jessop, F. E. Peters and M. R. Kessler, Cure kinetics characterization and monitoring of an epoxy resin using DSC, Raman spectroscopy, and DEA, *Compos. Part A Appl. Sci. Manuf.*, 2013, **49**, 100–108.

46 R. E. Lyon, K. E. Chike and S. M. Angel, In situ cure monitoring of epoxy resins using fiber-optic Raman spectroscopy, *J. Appl. Polym. Sci.*, 1994, **53**, 1805–1812.

47 S. Hu, X. Chen and J. M. Torkelson, Biobased Reprocessable Polyhydroxyurethane Networks: Full Recovery of Crosslink Density with Three Concurrent Dynamic Chemistries, *ACS Sustain. Chem. Eng.*, 2019, **7**, 10025–10034.

48 S. Doley, A. Bora, P. Saikia, S. Ahmed and S. K. Dolui, Blending of cyclic carbonate based on soybean oil and glycerol: a non-isocyanate approach towards the synthesis of polyurethane with high performance, *J. Polym. Res.*, 2021, **28**, 30–33.

49 V. Besse, F. Camara, F. Méchin, E. Fleury, S. Caillol, J. P. Pascault and B. Boutevin, How to explain low molar masses in PolyHydroxyUrethanes (PHUs), *Eur. Polym. J.*, 2015, **71**, 1–11.

50 X. Chen, L. Li, K. Jin and J. M. Torkelson, Reprocessable polyhydroxyurethane networks exhibiting full property recovery and concurrent associative and dissociative dynamic chemistry: Via transcarbamoylation and reversible cyclic carbonate aminolysis, *Polym. Chem.*, 2017, **8**, 6349–6355.

51 F. I. Altuna, V. Pettarin and R. J. J. Williams, Self-healable polymer networks based on the cross-linking of epoxidised soybean oil by an aqueous citric acid solution, *Green Chem.*, 2013, **15**, 3360–3366.

52 C. M. Tung and P. J. Dynes, Relationship between viscoelastic properties and gelation in thermosetting systems, *J. Appl. Polym. Sci.*, 1982, **27**, 569–574.

53 T. Vidil, F. Tournilhac, S. Musso, A. Robisson and L. Leibler, Control of reactions and network structures of epoxy thermosets, *Prog. Polym. Sci.*, 2016, **62**, 126–179.

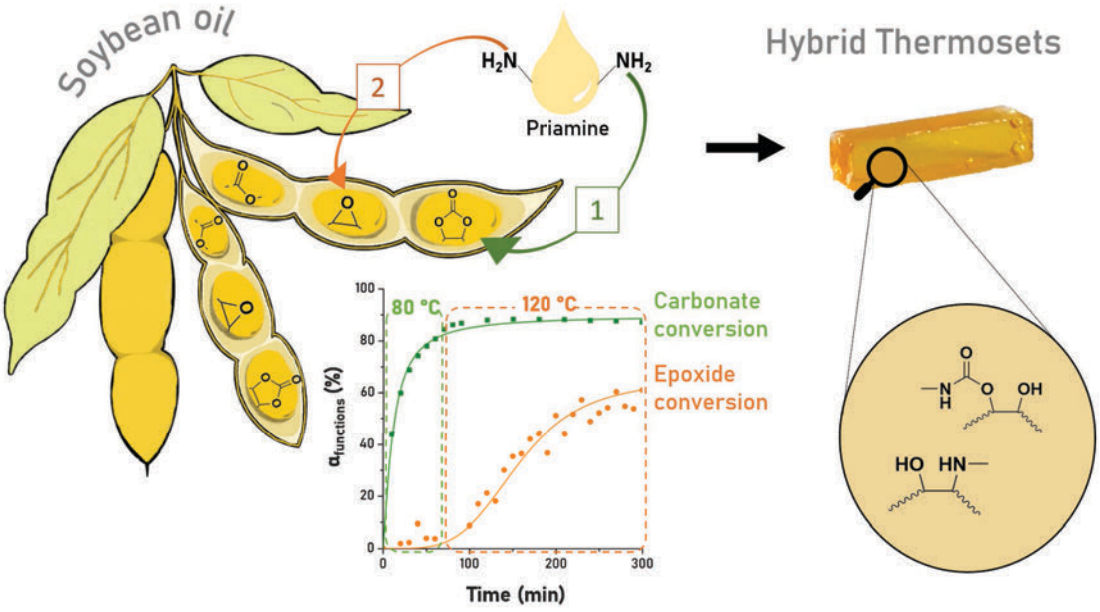

For table of contents only

Electronic Supplementary Material (ESI) for article published in *Polymer Chemistry* (2023)
DOI: https://doi.org/10.1039/D2PY01318E

ELECTRONIC SUPPORTING INFORMATION

Unveiling the reactivity of epoxides in carbonated epoxidized soybean oil and application to the stepwise synthesis of hybrid poly(hydroxyurethane) thermosets

P. Helbling[1,2], F. Hermant[2], M. Petit[2], T. Tassaing[3], T. Vidil[1*] and H. Cramail[1*]
[1]Univ. Bordeaux, CNRS, Bordeaux INP, LCPO, 16 avenue Pey-Berland 33600 Pessac, France
[2]Saint-Gobain Recherche Paris, 39 Quai Lucien Lefranc 93300 Aubervilliers, France
[3]Univ. Bordeaux, CNRS, ISM, 351 cours de la Libération 33400 Talence, France

TABLE OF CONTENTS

Characterization

Nuclear Magnetic Resonance (NMR): ^{1}H NMR spectra were recorded on a Bruker Advance 400 spectrometer (400.20 MHz) at room temperature. DMSO-d_6 and CD_2Cl_2 were used as deuterated solvents and 1,2,4-trichlorobenzene was used as an internal reference.

Infrared spectroscopy: Fourier transform infrared (FTIR) spectra were recorded on a Bruker-VERTEX 70 instrument (400 to 4000 cm^{-1}, 4 cm^{-1} resolution, 32 scans, DLaTGS MIR) equipped with a Pike GladiATR optical design (diamond crystal) for attenuated total reflectance (ATR). In the case of *in-situ* monitoring, the spectrometer was equipped with a thermally controlled diamond plate surrounded by a metallic piece creating a leak-proof cavity in order to proceed to the crosslinking reaction directly on the plate.

Raman spectroscopy: Raman measurements were performed with a XploRA spectrometer from Horiba using a laser source operating at 30 mW output power with a 785 nm excitation wavelength (260 to 2600 cm^{-1}, 6 cm^{-1} resolution, 600 lines mm^{-1}). In order to obtain a good signal to noise ratio, each spectrum resulted from the average of 12 or 24 accumulated scans with an integration time for each scan of about 10 seconds. A homemade stainless-steel cell equipped with a sapphire window was used to collect the Raman spectra during the crosslinking reactions, the laser beam being focused at the sample/sapphire window interface with the confocal microscope (X10 objective).

Rheological analyses: Rheological monitoring of the crosslinking reactions was performed using an Anton Paar MCR 302 rheometer equipped with disposable parallel plates (Ø = 25 mm) and operating in the multiwave mode using Fourier transform mechanical spectroscopy (FTMS).[41] A multiwave strain signal of 1 % amplitude for the 1 rad s^{-1} component was applied in order to collect G' and G'' data every 5 minutes for the 7 following frequencies: 1, 3, 6, 10, 30, 60 and 100 rad s^{-1}.

Thermogravimetric analysis (TGA): The thermal decomposition of the polymer networks was studied using a TA Instruments Q50. The samples were, in a first time, heated from 20 to 600 °C under a nitrogen atmosphere at a rate of 10 °C min^{-1} and then heated until 700 °C under air atmosphere.

Differential scanning calorimetry (DSC): Differential scanning calorimetry thermograms were recorded on a TA instrument DSC Q100. The samples, whose mass is comprised between 3 and 9.5 mg, were sealed in aluminium pans and analysed under nitrogen atmosphere. Two cycles were performed: a first one from -75 °C to 180 °C at a rate of 10 °C min^{-1} and a second one from -75 °C to 220 °C. The glass transition temperature (T_g) was measured from the latter.

Size exclusion chromatography (SEC): Polymer molar masses were determined by SEC using dimethylformamide (DMF + lithium bromide LiBr 1 g L^{-1}) as the eluent. Measurements were performed on an Ultimate 3000 system from Thermoscientific equipped with a diode array detector (DAD). A multi-angles laser light scattering detector (MALLS) and differential refractive index detector (dRI)

from Wyatt technology are also included. Species were separated on two Shodex Asahipack gel columns GF310 and GF510 (300 x 7.5 mm - exclusion limits from 500 Da to 300000 Da) at a flowrate of 0.5 mL min^{-1}. The temperature of the columns was held at 50 °C. Easivial Polystyrene kit from Agilent was used for the standards (M_n from 162 to 364 000 Da).

Synthesis of partially carbonated ESBO: CSBOX

A first range of experiments was carried out in order to optimize the parameters for the carbonation reactions. To this end the influence of the temperature, the initial pressure of CO_2, the amount of catalyst, and the stirring mode was studied by measuring the conversion of epoxides into carbonates X – in other words the carbonate ratio – after a reaction time of 24 or 72 hours. Figure S1 represents the evolution of X as a function of the various parameters of the reaction. For each experiment, X is measured at the end of the reaction according to ^{1}H NMR analyses (see Figure S3). The temperature as well as the amount of catalyst have a significant impact on X, as already illustrated by different authors.[1,2] Increasing the temperature from 80 °C to 120 °C results in an increase of X from 34 % to 99 % (Figure S1a). The use of the catalyst TBABr is necessary as the catalyst-free reaction does not proceed (Figure S1b). Furthermore, an increase of the catalyst content from 1.5 to 3 wt% fostered the conversion from 50 % up to 80 %. Increasing the stirring from 250 to 500 rpm (Figure S1c) or the initial pressure of CO_2 from 25 to 45 bar (Figure S1d) has no significant impact on X.

In the end, after taking into account the influence of each parameter, the carbonation reactions were carried out at 120 °C under a 250 rpm magnetic stirring with an initial pressure of CO_2 of 45 bar and a catalyst content of 3 wt%.

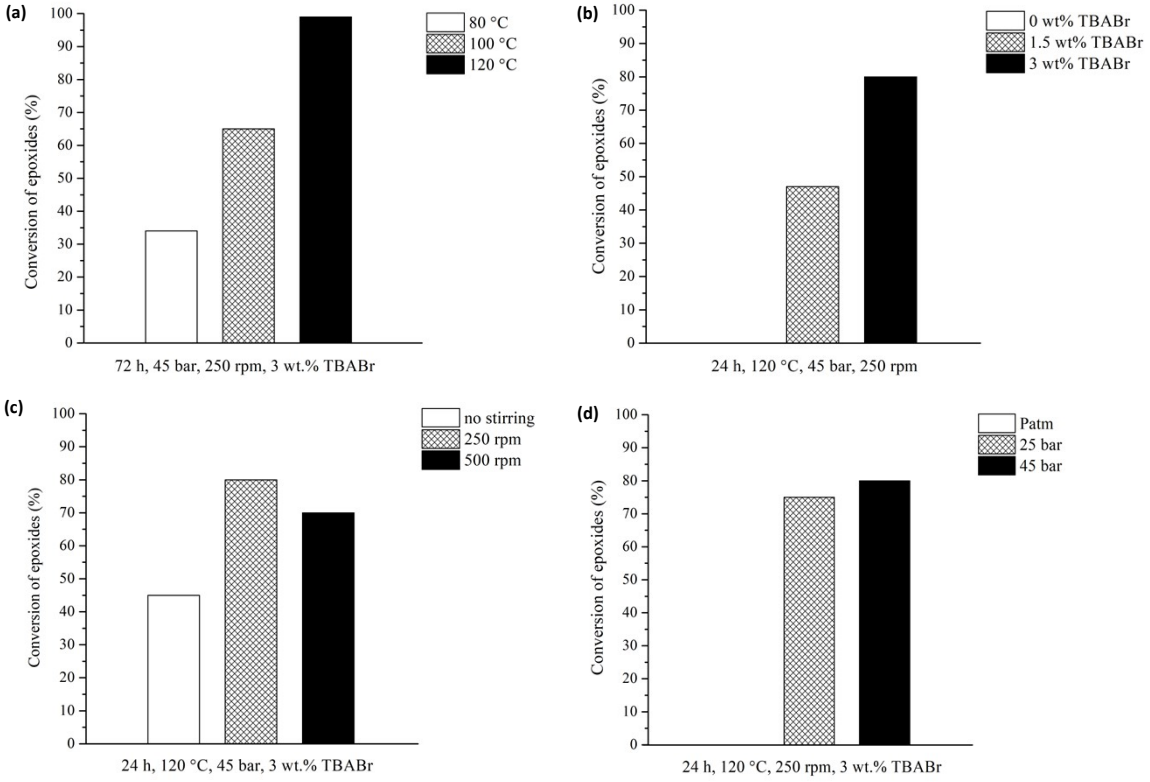

Figure S1: Conversion of epoxides, X, during carbonation reactions depending on the parameters: a) temperature, b) amount of catalyst, c) stirring mode and d) initial pressure of CO2

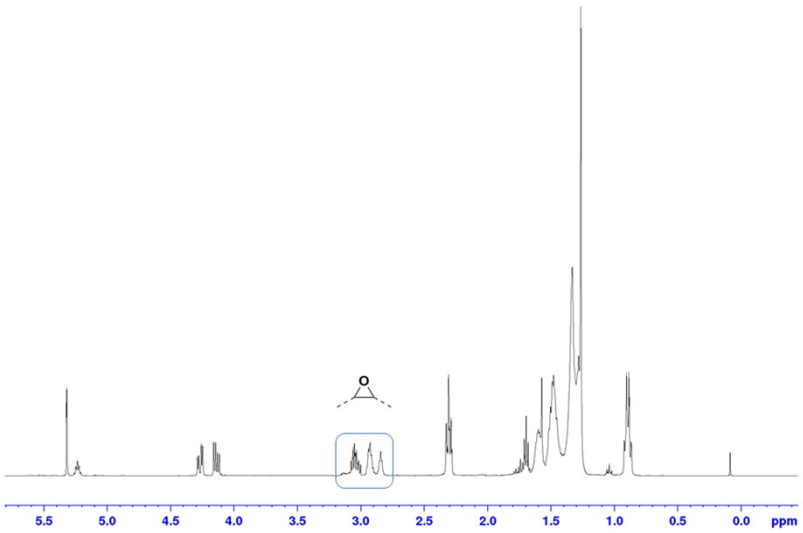

Figure S2: ^{1}H NMR spectrum of ESBO in CD_2Cl_2

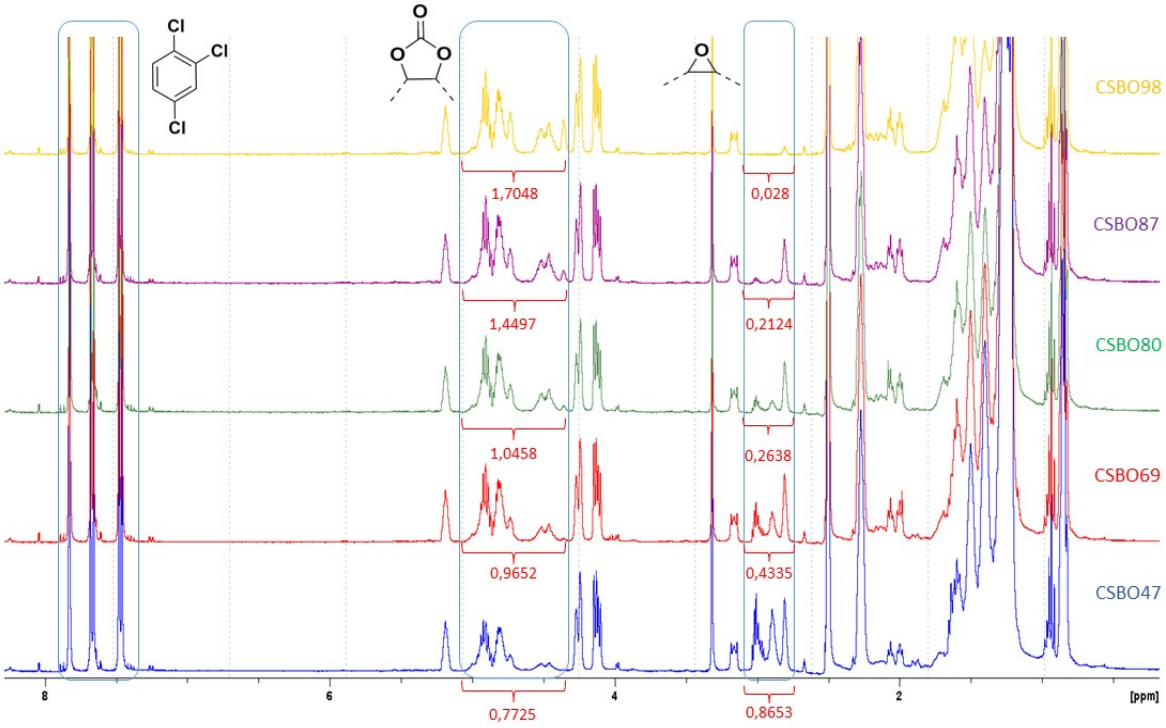

Figure S3: Overlay of ^{1}H NMR spectra in DMSO-d_6 of partially carbonated epoxidised soybean oils which X is comprised between 47 and 98 %

Method for NMR integration:

The signal associated with the reference protons of 1,2,4-trichlorobenzene are integrated as 3 protons.

Considering the conversion of epoxides into carbonate as the only reaction occurring, (**Eq. S*1*** was used to calculate the conversion of epoxides into carbonates, X, for each carbonation reaction:

$$X\,(\%) = \frac{\int H_{carbonate}}{\int H_{carbonate} + \int H_{epoxide}}$$

(Eq. S1)

with $\int H_{epoxide}$ and $\int H_{carbonate}$ the integrals of the peaks associated with the 2 protons of epoxide and carbonate functions respectively.

(**Eq. S2** was then used to calculate $C_{carbonate}$ as the number of moles of cyclic carbonate per kilogram of a partially carbonated soybean oil CSBOX :

$$C_{carbonate}\left(mol\ kg^{-1}\right) = \frac{\int H_{carbonate}}{2} \times n_{REF} \times \frac{1000}{m_{CSBOx}}$$

(Eq. S2)

with $\int H_{carbonate}$ the integral of the peaks associated with the 2 protons of carbonate functions, n_{ref} the number of moles of internal reference and m_{CSBOx} the mass of partially carbonated soybean oil used for the analysis.

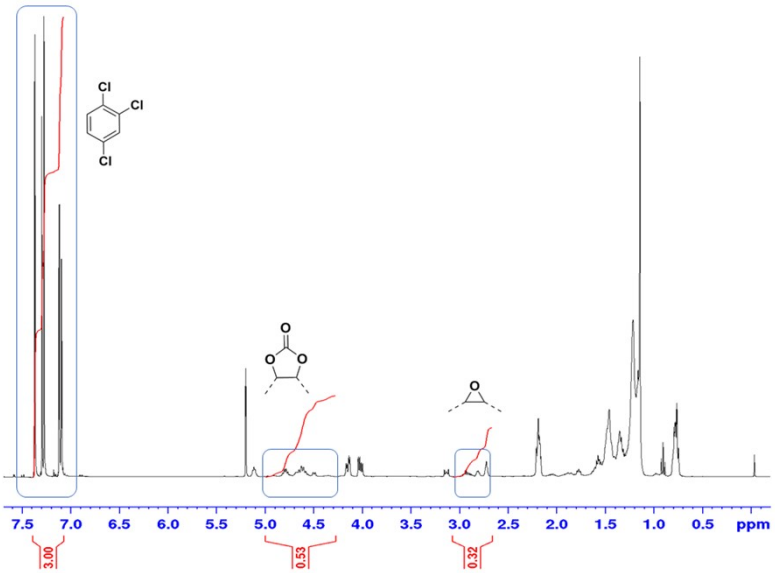

Figure S4: ^1H NMR spectrum of CSBO45 in CD_2Cl_2

Dual-spectroscopic investigation of the crosslinking reaction of CSBO45

Methods used to follow the conversion of reactive functions of CSBO45:

In the case of *in-situ* IR spectroscopy monitoring, the conversion of the carbonate and ester functions was followed thanks to the disappearance of their carbonyl related absorbance bands, respectively at 1808 and 1744 cm^{-1}. The absorbance band at 2920 cm^{-1}, related to the C-H of the aliphatic chains, was chosen as an internal standard. Conversions $\alpha_{function}$ (%) of either carbonates or esters were determined thanks to Equation S(**Eq. S*3*** following the Beer-Lambert law from the change of normalized absorbance at 1808 and 1744 cm^{-1}:

$$\alpha_{function}(\%) = \left(1 - \frac{\bar{A}^{t}_{function}}{\bar{A}^{0}_{function}}\right) \times 100 \quad \textbf{(Eq. S3)}$$

where $\bar{A}^{0}_{function} = \frac{A^{0}_{function}}{A^{0}_{2920}}$ and $\bar{A}^{t}_{function} = \frac{A^{t}_{function}}{A^{t}_{2920}}$ are the normalized absorbance of the function studied before curing and after the reaction time t respectively.

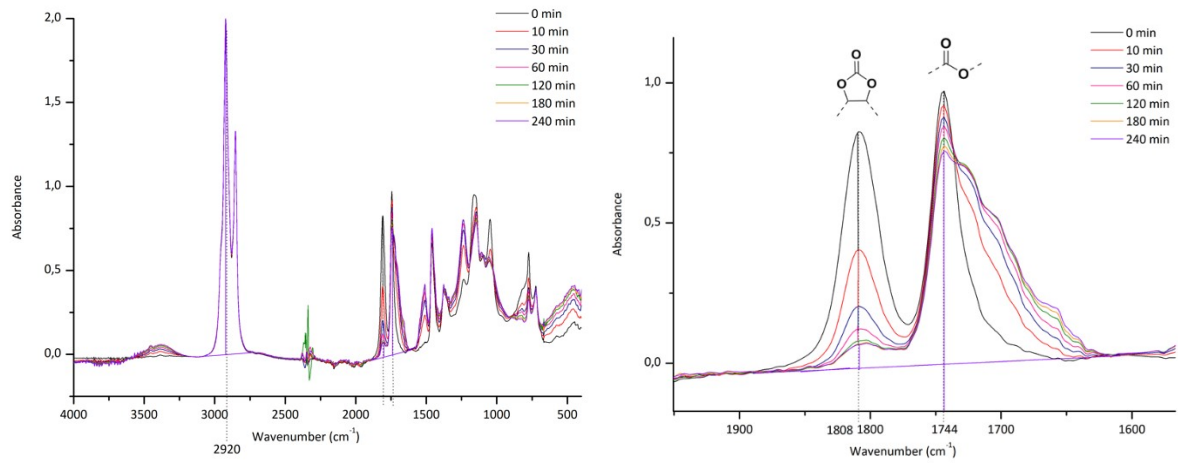

Figure S5: Overlay of IR spectra and zoom on the 1650-1950 cm^{-1} window from the monitoring of the 4 h curing at 120 °C of CSBO45-Priamine 1075 system

In the case of in-situ Raman spectroscopy monitoring, the sample was poured into a closed cell adapted to the spectrometer and then heated to the desired temperature. The conversion of the epoxide functions was determined thanks to the disappearance of the band at 1267 cm^{-1} comparatively to the band at 1440 cm^{-1}, chosen as an internal standard. In this case, the conversion of epoxides was determined by Equation S(**Eq. S**4 :

$$\alpha_{epoxide}(\%) = \left(1 - \frac{\bar{A}^{t}_{epoxide}}{\bar{A}^{0}_{epoxide}}\right) \times 100 \quad \textbf{(Eq. S)}$$

where $\bar{A}^{0}_{epoxide} = \frac{A^{0}_{epoxide}}{A^{0}_{1440}}$ and $\bar{A}^{t}_{function} = \frac{A^{t}_{epoxide}}{A^{t}_{1440}}$ are the normalized absorbance of the function studied before curing and after the reaction time t respectively.

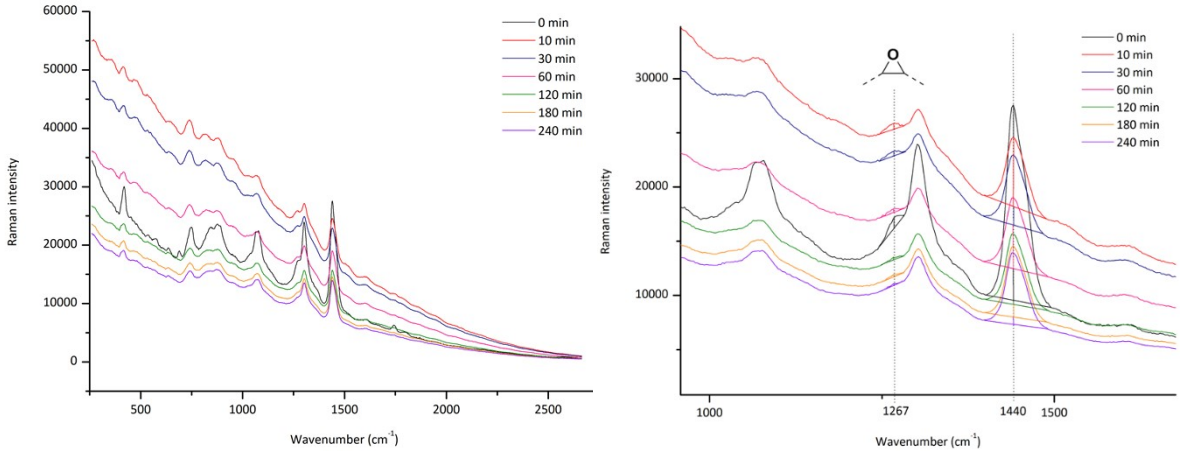

Figure S6: Overlay of Raman spectra and zoom on the 1000-1600 cm^{-1} zone from the monitoring of the 4 h curing at 120 °C of CSBO45-Priamine 1075 system

Methods used to follow the gelation of the polymers by rheology:

The gel point, t_{gel}, was defined as the moment when Winter and Chambon criterion was met, that is to say:

$$G'(\omega) \sim G''(\omega) \sim \omega^{n}$$

where G' and G'' are the storage and loss modulus, respectively, and ω the angular frequency.

More precisely, t_{gel} was the moment when G' and G'' curves as function of ω were linear and parallel in logarithmic scale with a slope equal to n. In the end, t_{gel} can also be determined thanks to the loss factor tan(δ) plotted as a function of time. t_{gel} would be the moment when all the representative curves of tan(δ) for various ω meet.

Conversion of reactive functions for CSBO45 – Priamine 1075 reactions:

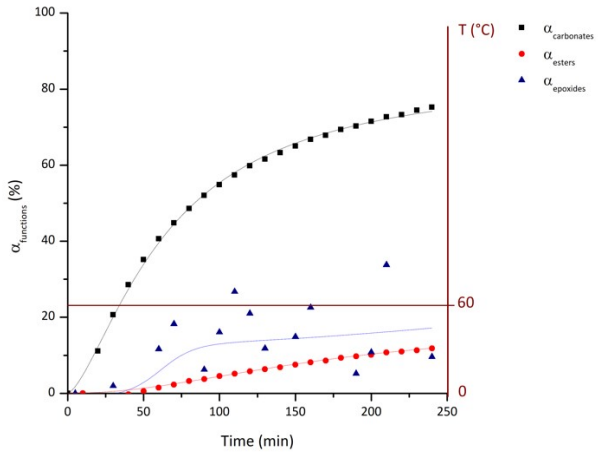

Figure S7: Conversion curves of carbonates (black), esters (red) and epoxides (blue) as a function of time for the 4 h curing at T = 60 °C of CSBO45-Priamine 1075

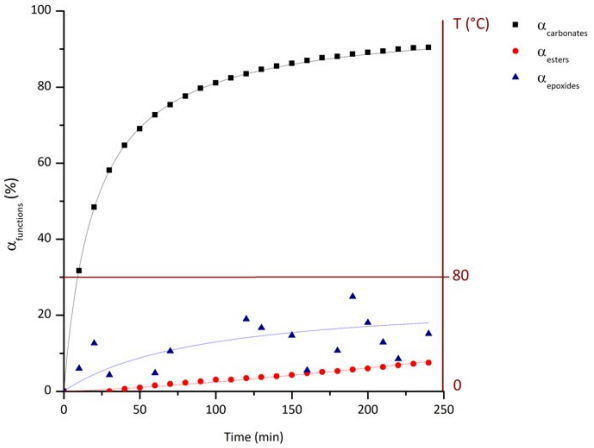

Figure S8: Conversion curves of carbonates (black), esters (red) and epoxides (blue) as a function of time for the 4 h curing at T = 80 °C of CSBO45-Priamine 1075

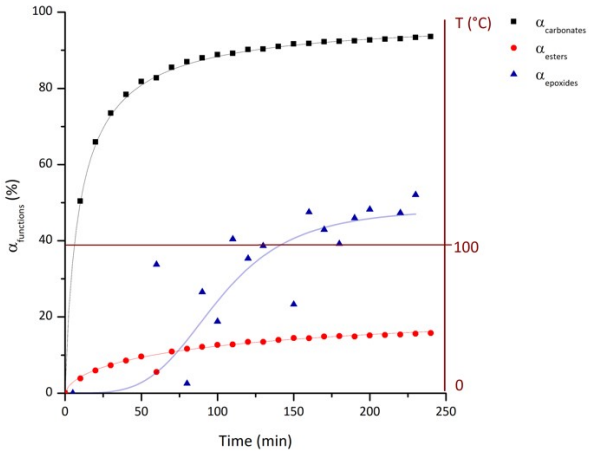

Figure S9: Conversion curves of carbonates (black), esters (red) and epoxides (blue) as a function of time for the 4 h curing at T = 100 °C of CSBO45-Priamine 1075

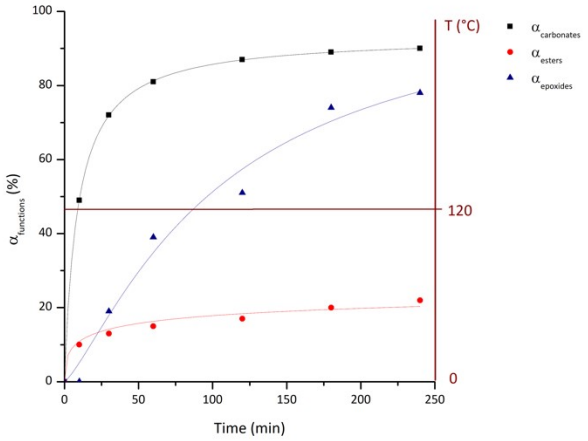

Figure S10: Conversion curves of carbonates (black), esters (red) and epoxides (blue) as a function of time for the 4 h curing at T = 120 °C of CSBO45-Priamine 1075

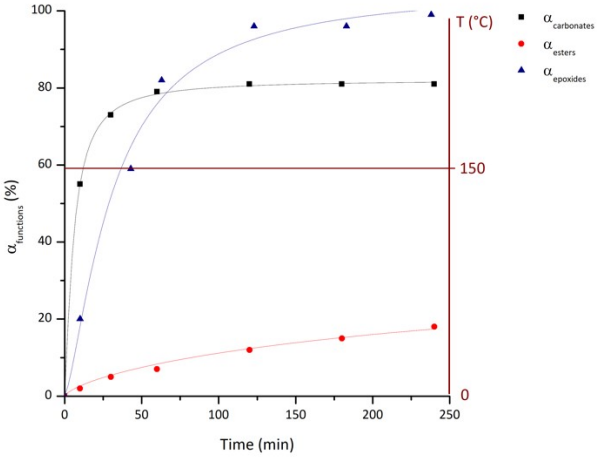

Figure S11: Conversion curves of carbonates (black), esters (red) and epoxides (blue) as a function of time for the 4 h curing at T = 150 °C of CSBO45-Priamine 1075

Conversion of reactive functions for CSBO45 – 8DA reactions:

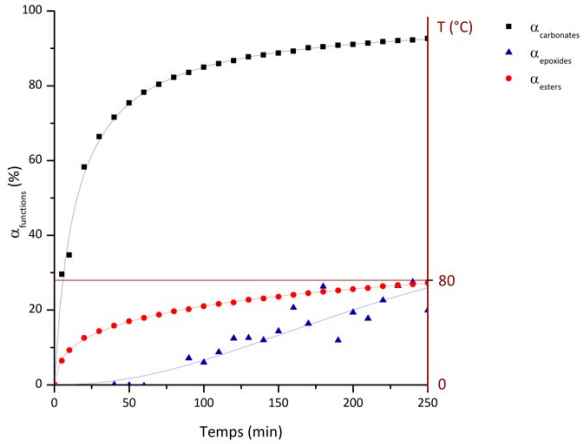

Figure S12: Conversion curves of carbonates (black), esters (red) and epoxides (blue) as a function of time for the 4 h curing at T = 80 °C of CSBO45-8DA

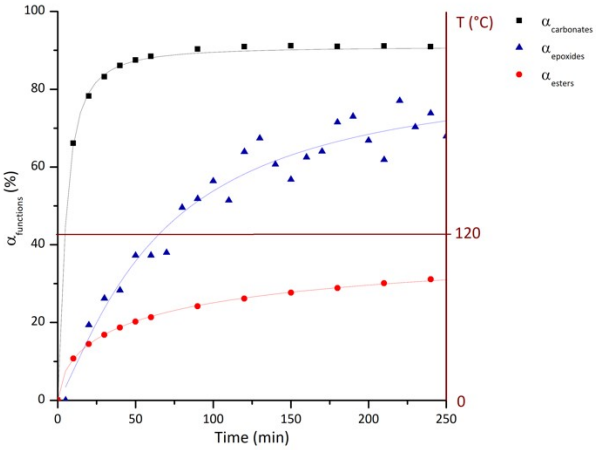

Figure S13: Conversion curves of carbonates (black), esters (red) and epoxides (blue) as a function of time for the 4 h curing at T = 120 °C of CSBO45-8DA

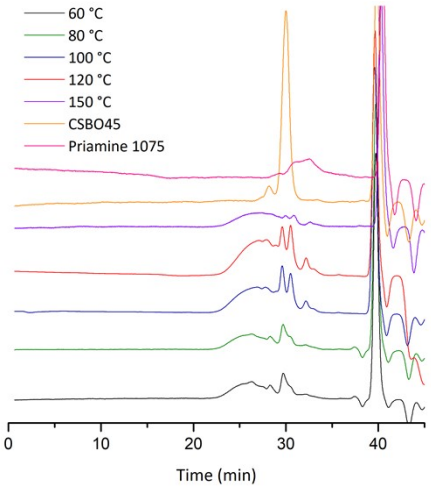

Figure S14: Overlay of SEC traces of the soluble fraction of CSBO45+Priamine 1075-based polymers cured for 4 h at 60, 80, 100, 120 and 150 °C respectively and of both reactants

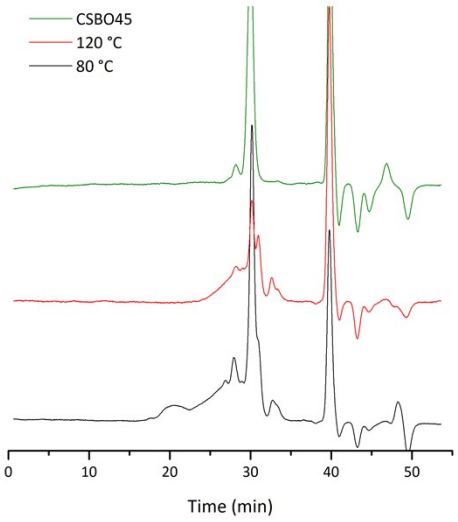

Figure S15: Overlay of SEC traces of the soluble fraction of CSBO45+8DA-based polymers cured for 4 h at 80 and 120 °C respectively and of CSBO45

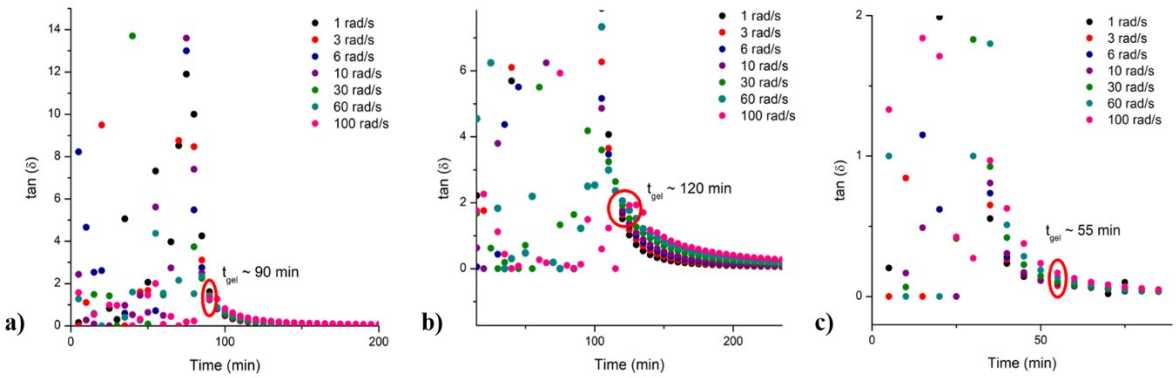

Figure S16: Tan(δ) curves as a function of time recorded at various angular frequencies during rheological monitoring of a) CSBO45-Priamine 1075 curing at 120 °C ; b) CSBO45-8DA curing at 80 °C ; c) CSBO45-8DA curing at 120 °C - gel points determined *via* the Winter and Chambon criterion

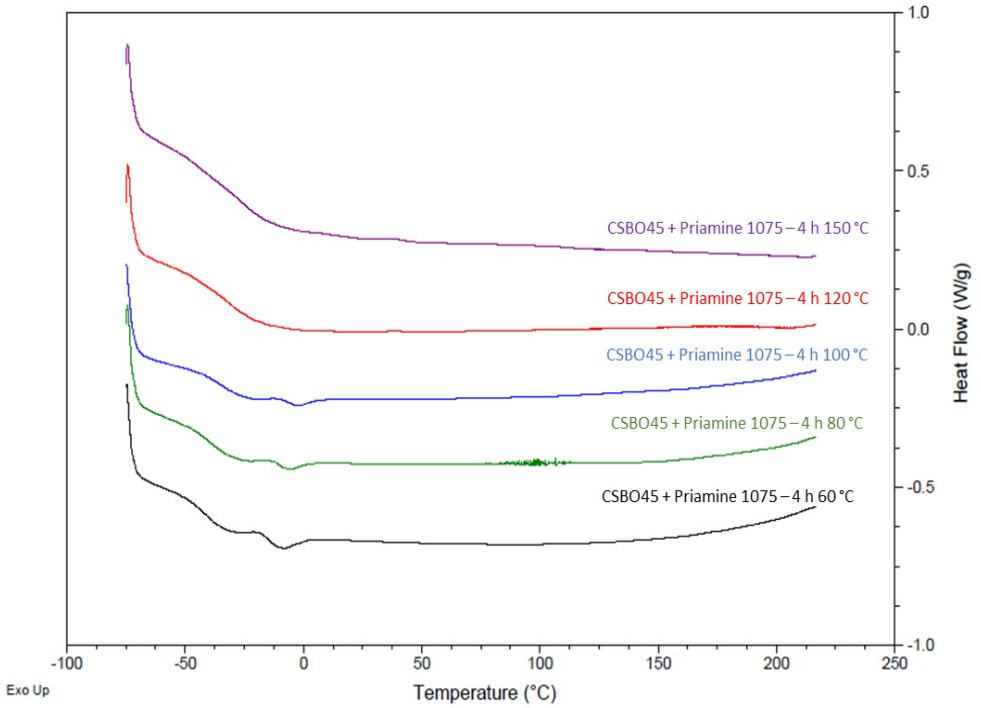

Figure S17: Overlay of DSC traces of CSBO45+Priamine 1075-based polymers cured for 4 h at 60, 80, 100, 120 and 150 °C respectively

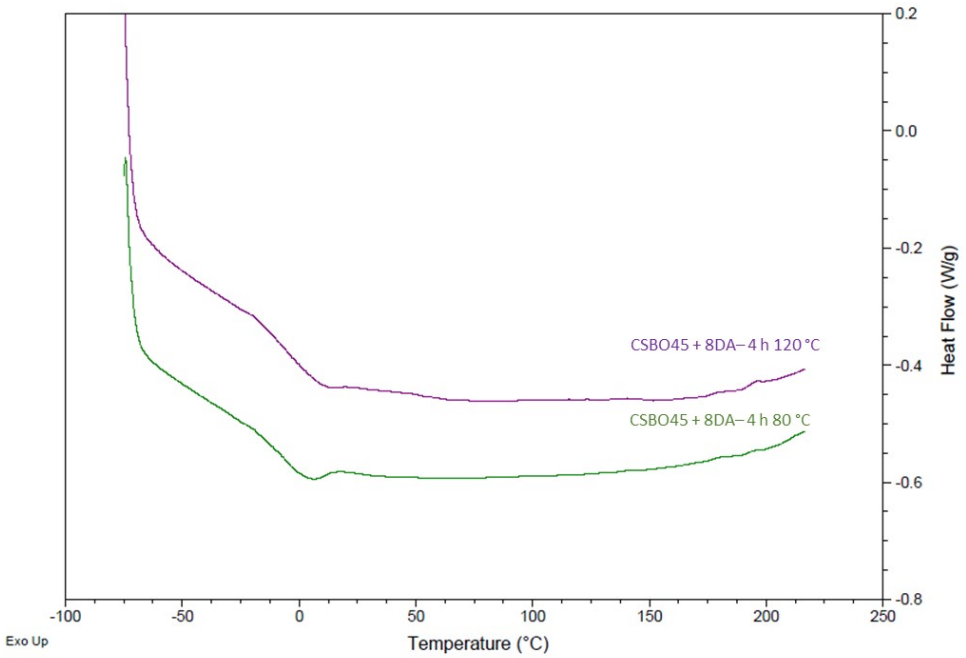

Figure S18: Overlay of DSC traces of CSBO45+8DA-based polymers cured for 4 h at 80 °C and 120 °C respectively

Crosslinking reactions of ESBO with Priamine

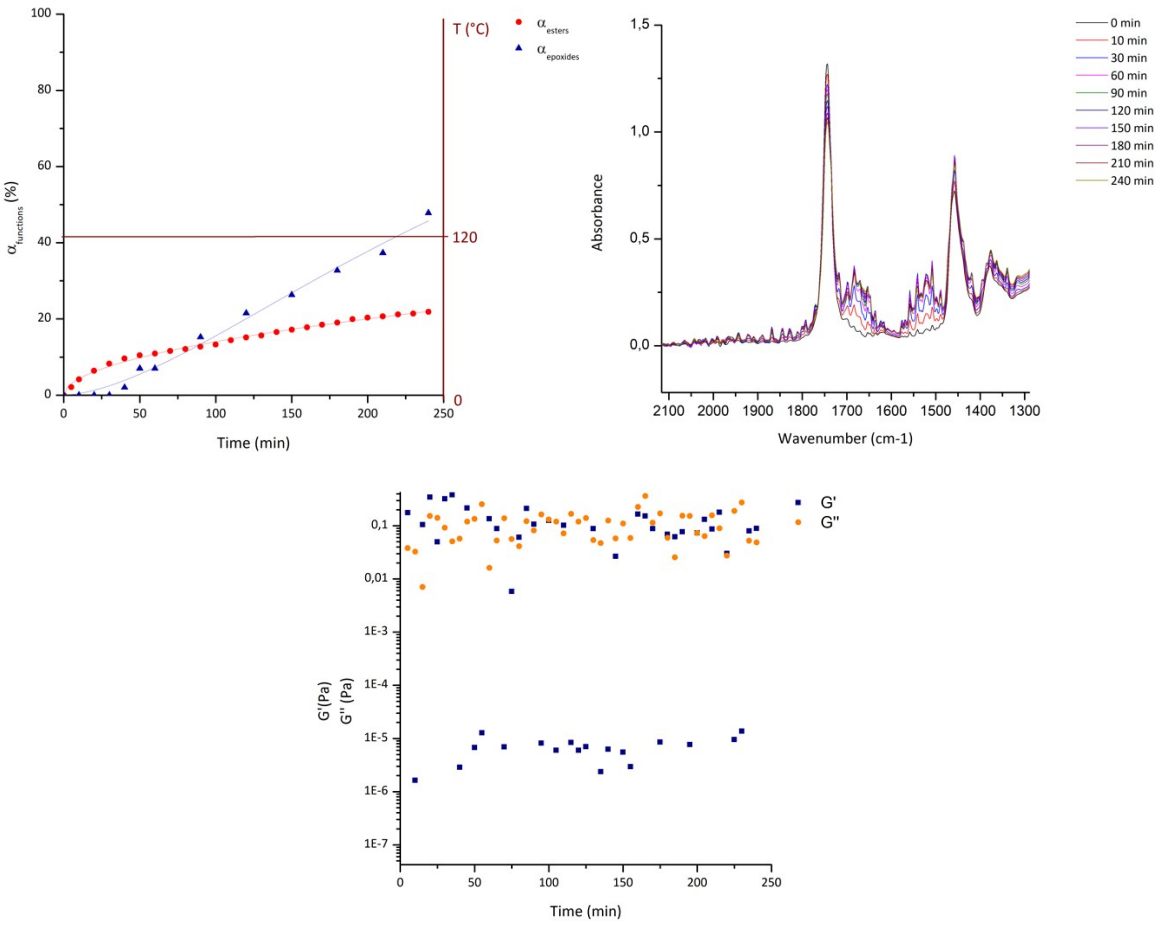

Figure S19: Conversion curves of esters (red) and epoxides (blue), IR spectra overlay and rheological monitoring of the 4 h curing at T = 120 °C of ESBO-Priamine 1075

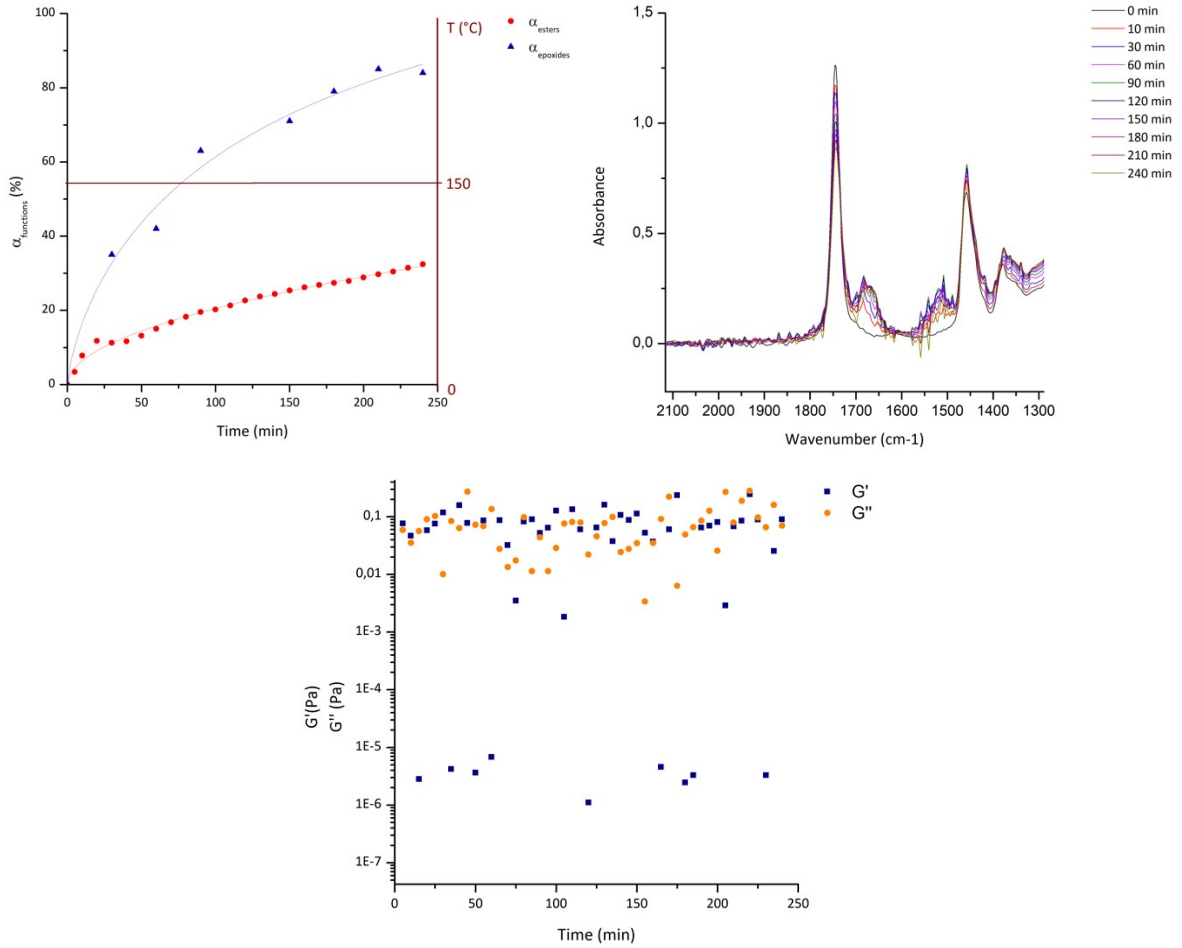

Figure S20: Conversion curves of esters (red) and epoxides (blue), IR spectra overlay and rheological monitoring of the 4 h curing at T = 150 °C of ESBO-Priamine 1075

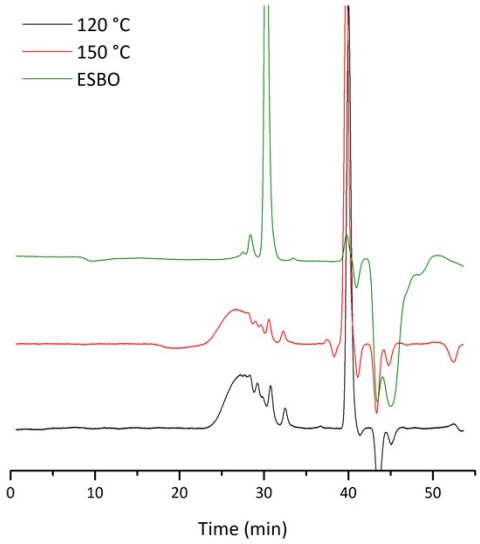

Figure S21: Overlay of SEC traces of ESBO+Priamine 1075-based polymers cured for 4 h at 120 and 150 °C respectively and of ESBO

Thermolatent systems based on CSBOX

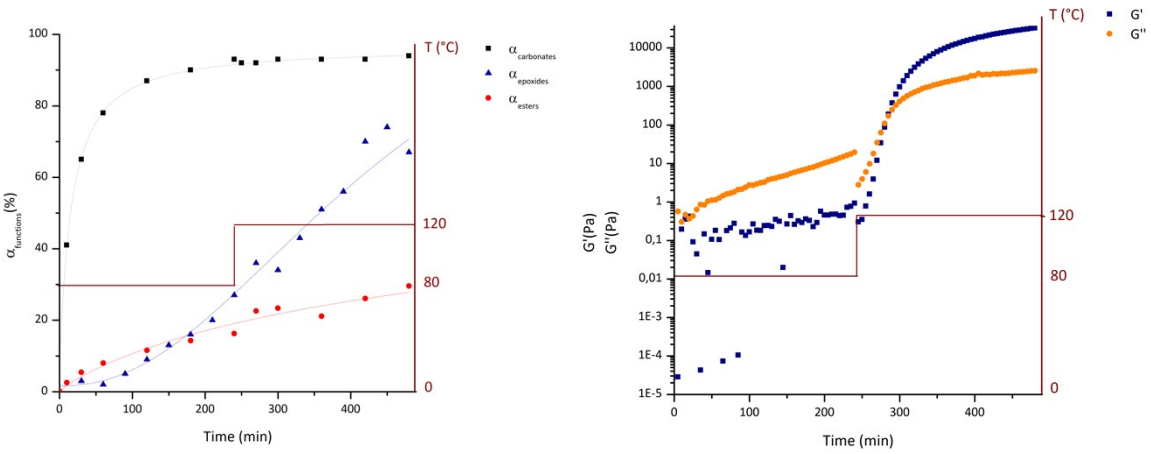

Figure S22: Conversion of carbonates (black), esters (red) and epoxides (blue) and rheological monitoring of the 2-step curing sequence (t_1 = 4 h, T_1 = 80 °C and t_2 = 4 h, T_2 = 120 °C) of CSBO45-Priamine 1075

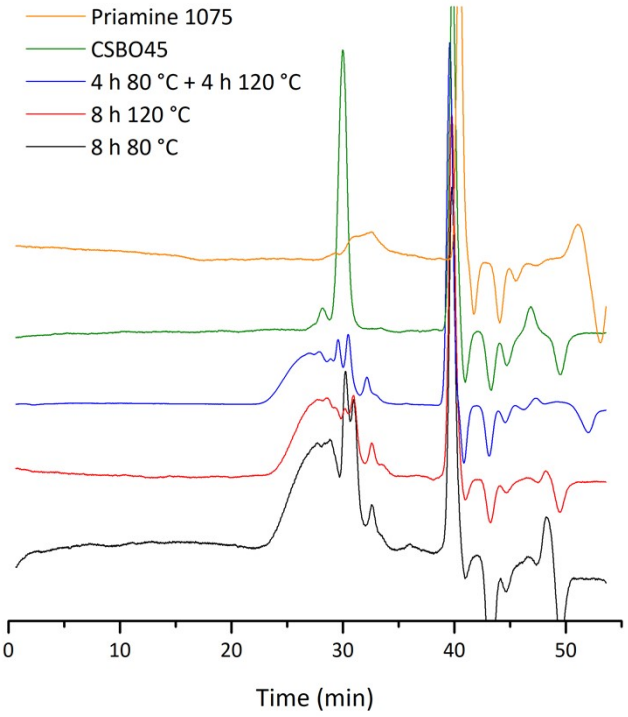

Figure S23: Overlay of SEC traces of the soluble fraction of CSBO45+Priamine 1075-based polymers cured for 8 h at 80 °C (black line) and 120 °C (red line) respectively, 4 h at 80 °C + 4 h at 120 °C (green line) and of both reactants

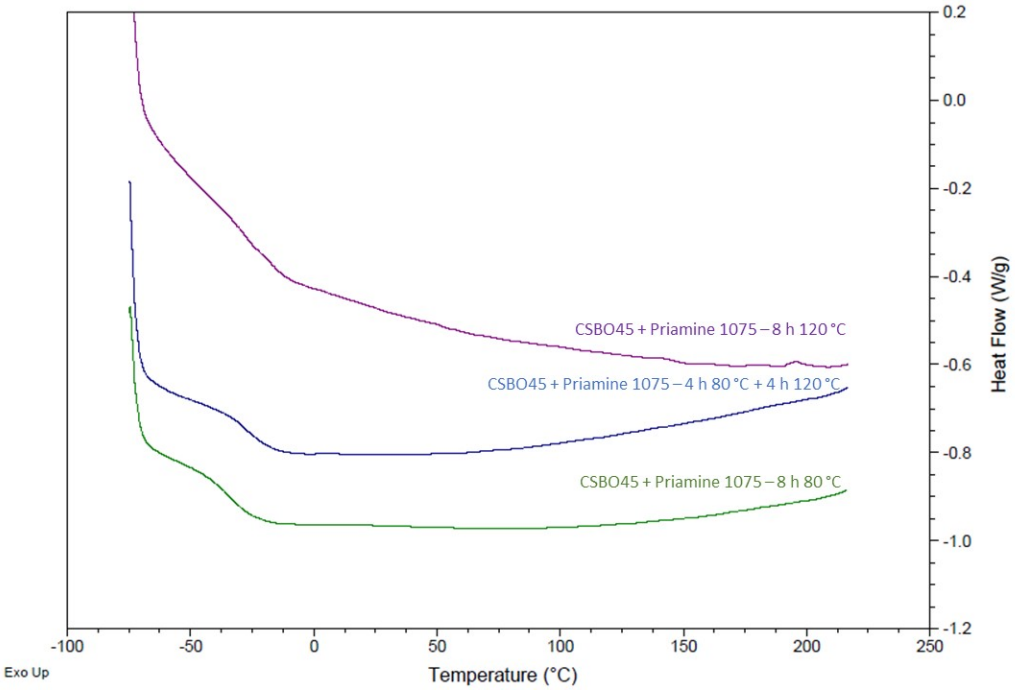

Figure S24: Overlay of DSC traces of CSBO45+Priamine 1075-based polymers cured for 8 h at 80 °C (green line) or 120 °C (purple line) respectively and 4 h at 80 °C + 4 h at 120 °C (blue line)

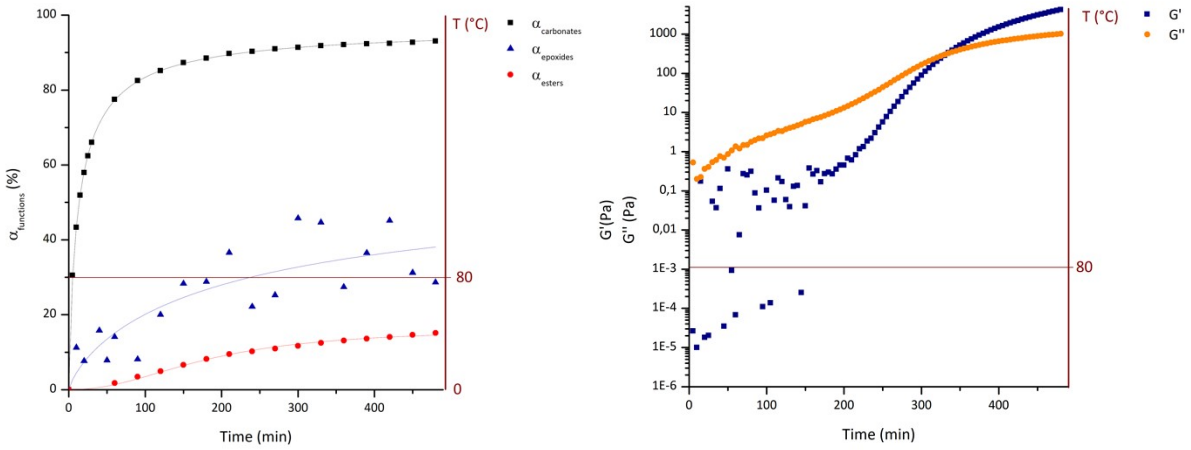

Figure S25: Conversion of carbonates (black), esters (red) and epoxides (blue) and rheological monitoring of the 8 h curing at T = 80 °C of CSBO45-Priamine 1075

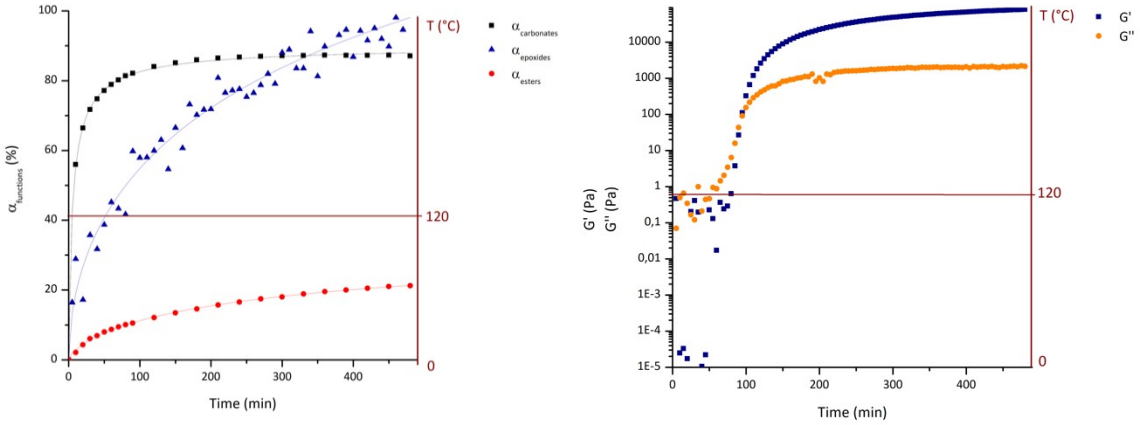

Figure S26: Conversion of carbonates (black), esters (red) and epoxides (blue) and rheological monitoring of the 8 h curing at T = 120 °C of CSBO45-Priamine 1075

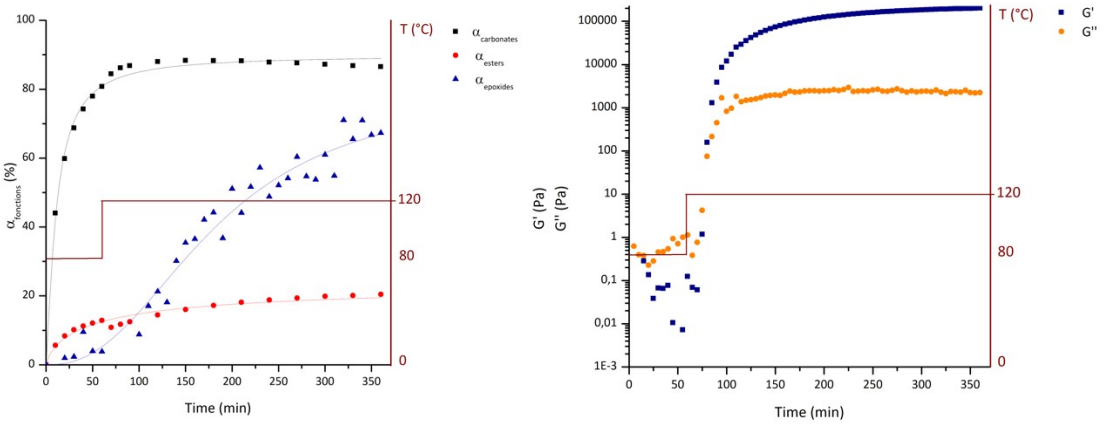

Figure S27: Conversion of carbonates (black), esters (red) and epoxides (blue) and rheological monitoring of the 2-step curing sequence (t_1 = 1 h, T_1 = 80 °C and t_2 = 5 h, T_2 = 120 °C) of CSBO45-8DA

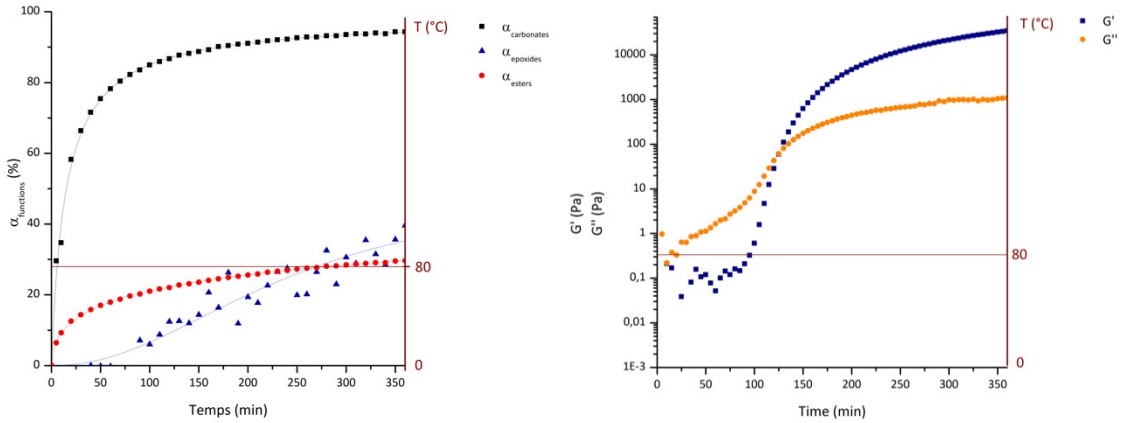

Figure S28: Conversion of carbonates (black), esters (red) and epoxides (blue) and rheological monitoring of the 6 h curing at T = 80 °C of CSBO45-8DA

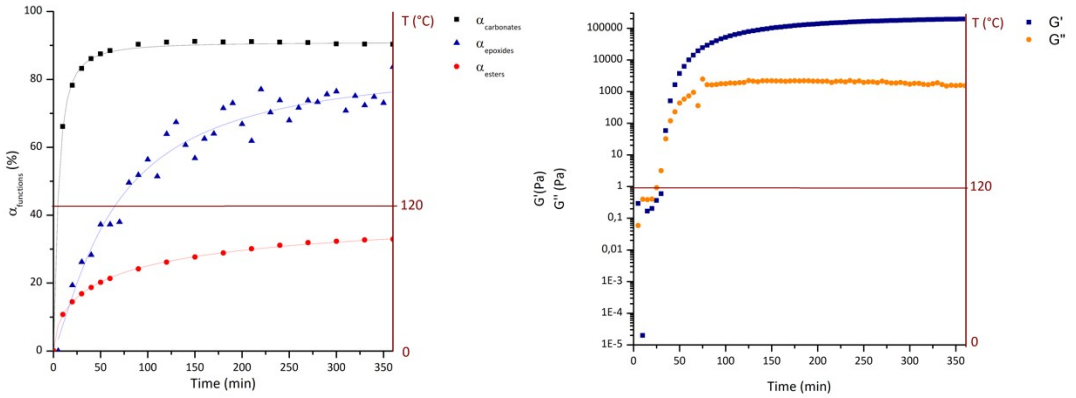

Figure S29: Conversion of carbonates (black), esters (red) and epoxides (blue) and rheological monitoring of the 6 h curing at T = 120 °C of CSBO45-8DA

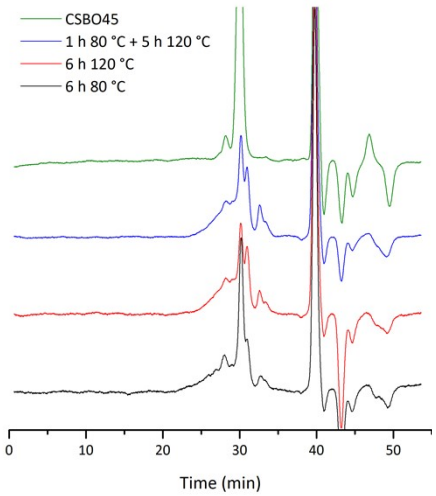

Figure S30: Overlay of SEC traces of the soluble fraction of the CSBO45+8DA-based polymers cured for 6 h at 80 °C (black line) and 120 °C (red line) respectively, 1 h at 80 °C + 5 h at 120 °C (blue line) and of CSBO45 (green line)

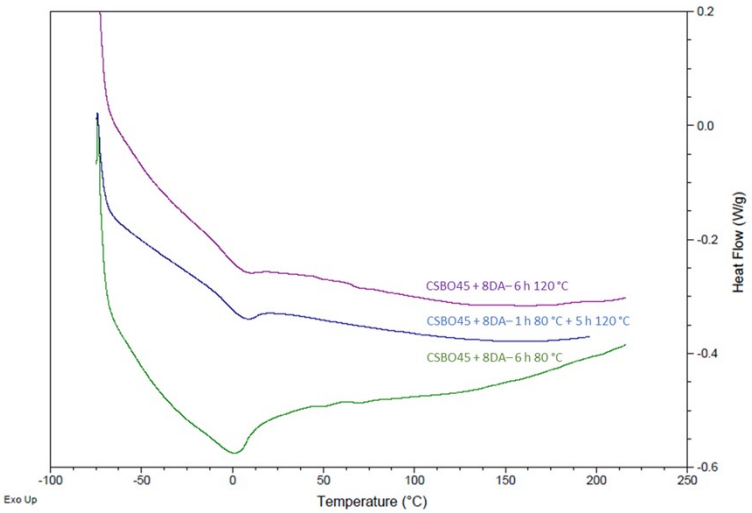

Figure S31: Overlay of DSC traces of CSBO45+8DA-based polymers cured for 6 h at 80 °C (green line) or 120 °C (purple line) respectively and 1 h at 80 °C + 5 h at 120 °C (blue line)

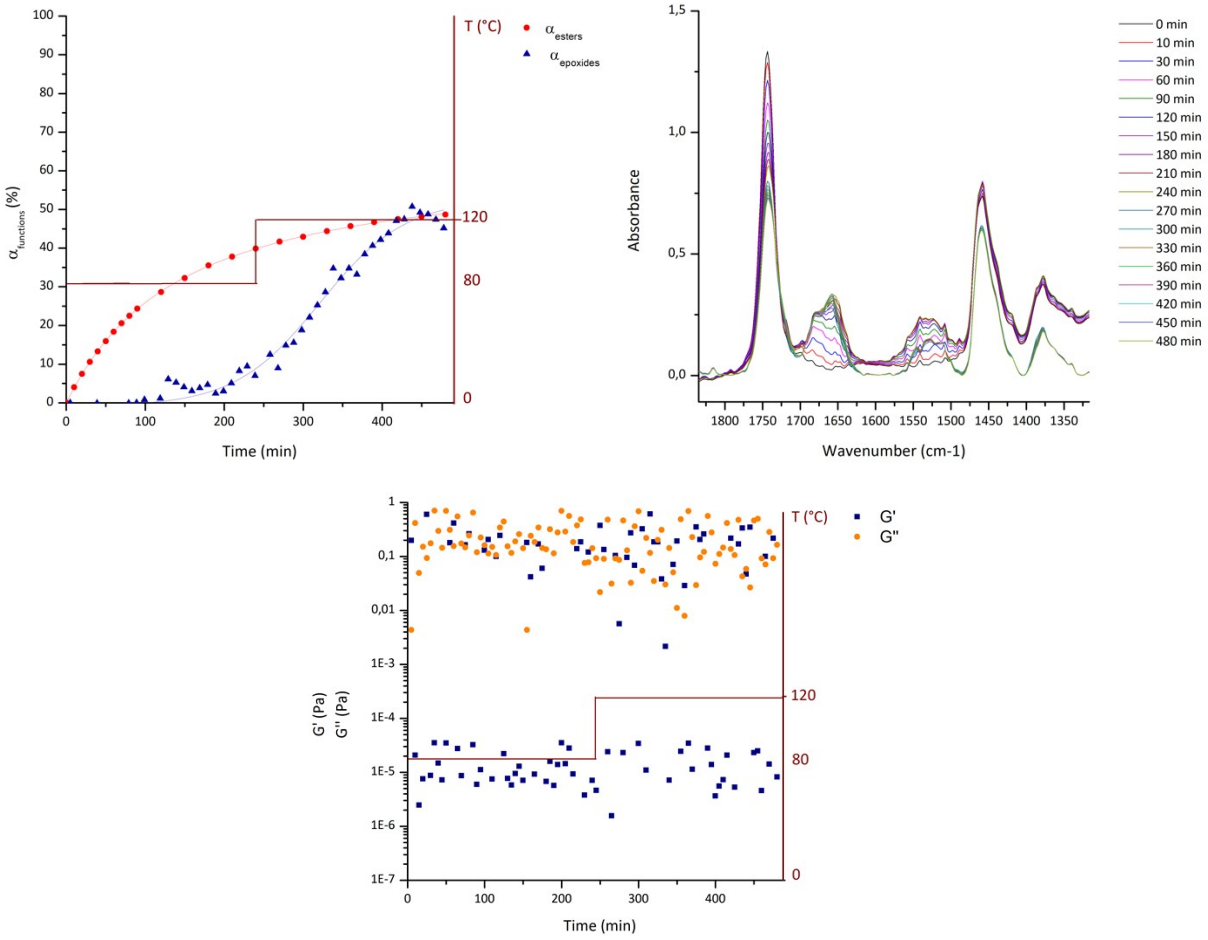

Figure S32: Conversion of esters (red) and epoxides (blue), overlay of IR spectra and rheological monitoring of the 2-step curing sequence ((t_1 = 4 h, T_1 = 80 °C and t_2 = 4 h, T_2 = 120 °C) of ESBO-Priamine 1075

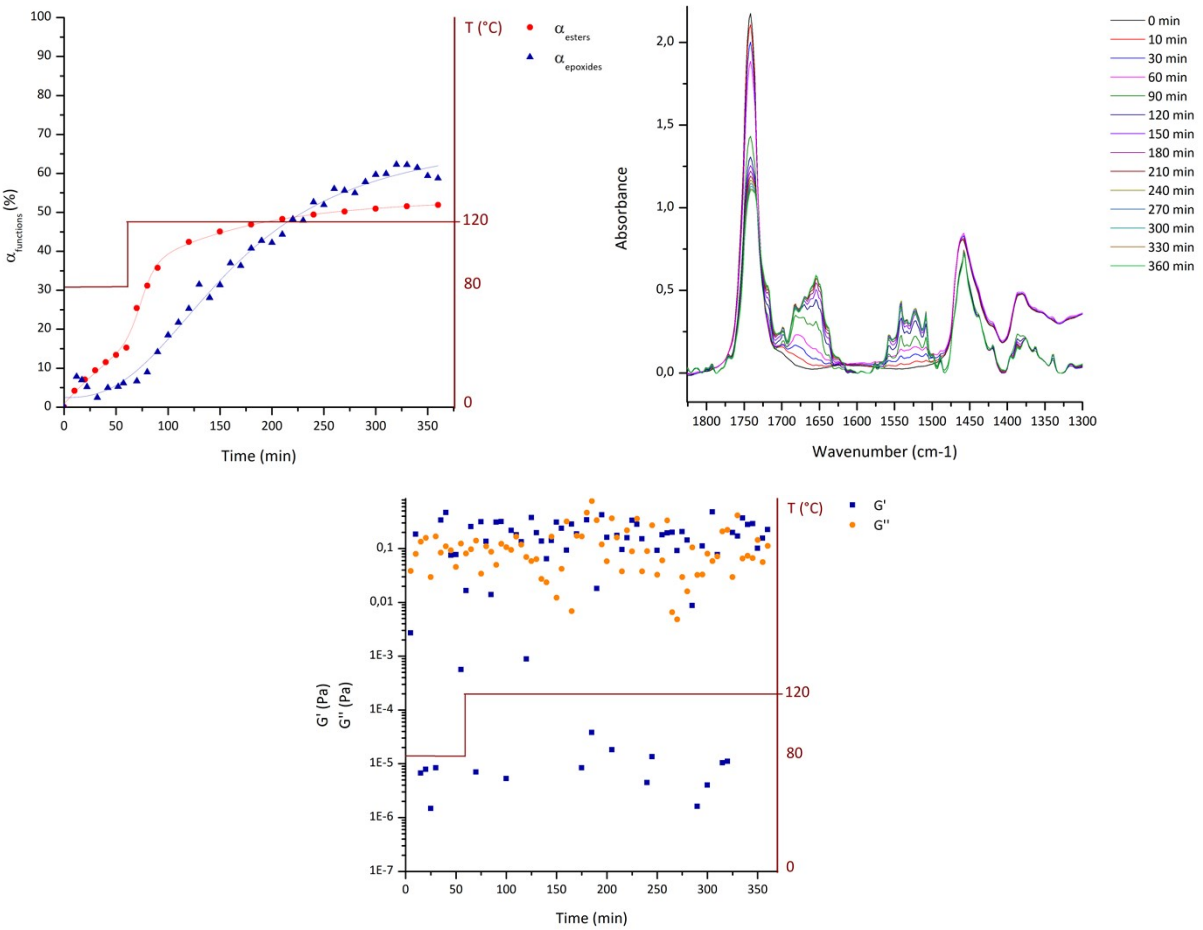

Figure S33: Conversion of esters (red) and epoxides (blue), overlay of IR spectra and rheological monitoring of the 2-step curing sequence (t_1 = 1 h, T_1 = 80 °C and t_2 = 5 h, T_2 = 120 °C) of ESBO-8DA

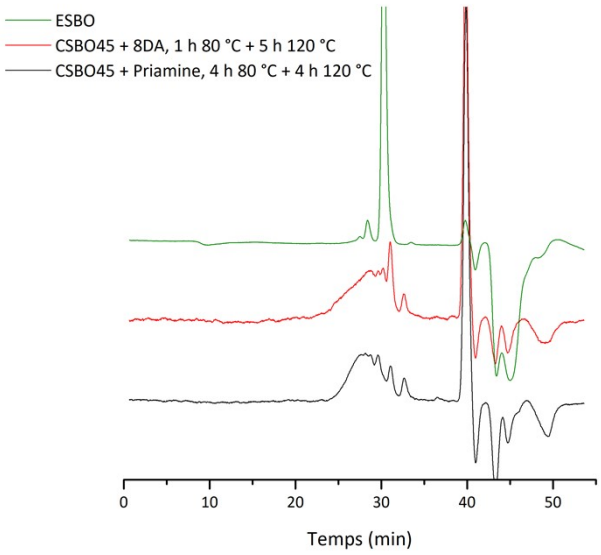

Figure S34: Overlay of SEC traces of ESBO (green line), ESBO-Priamine 1075-based polymer cured 4 h at 80 °C + 4 h at 120 °C (black line) and of ESBO-8DA-based polymer cured 1 h at 80 °C + 5 h at 120 °C (red line)

References

1 M. Bähr and R. Mülhaupt, Linseed and soybean oil-based polyurethanes prepared via the non-isocyanate route and catalytic carbon dioxide conversion, *Green Chem.*, 2012, **14**, 483–489.

2 S. Javni, I., Hong, D. P., Petrovic, Z., Soy-Based Polyurethanes by Nonisocyanate Route, *J. Appl. Polym. Sci.*, 2008, **108**, 3867–3875.